UNIVERSIDAD DE CONCEPCIÓN

Centro de Investigación en Ingeniería Matemática (CI^{2}MA)

A model of continuous sedimentation with compression and reactions

Raimund Bürger, Stefan Diehl,
Camilo Mejías

PREPRINT 2016-17

SERIE DE PRE-PUBLICACIONES

A MODEL OF CONTINUOUS SEDIMENTATION WITH COMPRESSION AND REACTIONS*

RAIMUND BÜRGER†, STEFAN DIEHL‡, AND CAMILO MEJÍAS†

Abstract. Continuously operated settling tanks are used for the gravity separation of solid-liquid suspensions in several industries. Mathematical models of these units have been a topic for well-posedness and numerical analysis even in one space dimension due to the spatially discontinuous coefficients of the underlying strongly degenerate parabolic, nonlinear model PDE. Such a model is extended to describe the sedimentation of multi-component particles that undergo reactions with several soluble constituents of the liquid phase. The fundamental equations are reformulated as a system of model PDEs for which a new numerical scheme is formulated. This scheme combines a difference scheme for conservation laws with discontinuous flux with an approach of numerical percentage propagation for multi-component flows. The main result is an invariant region property, which implies that physically relevant numerical solutions are produced. Simulations of denitrification in secondary settling tanks in wastewater treatment illustrate the model and its discretization.

Key words. activated sludge, clarifier-thickener, convection-diffusion-reaction PDE, degenerate parabolic conservation law, secondary settling tank, sedimentation with compression

AMS subject classifications. 35K57, 35K65, 35L65, 35Q35, 35R05

1. Introduction.

1.1. Scope. The separation of fine solid particles from a liquid by gravity under continuous flows in and out of large tanks is a common unit operation in wastewater treatment, mineral processing, hydrometallurgy, and other areas. Since gravity acts in one dimension and computational resources for simulations, mostly within larger systems, are limited, spatially one-dimensional models are widely used. In fact, the continuous sedimentation of a solid-liquid suspension subject to applied feed and bulk flows, hindered settling, and sediment compressibility (e.g., due to flocculation) can be described by a scalar, nonlinear, strongly degenerate parabolic PDE for the solids concentration $X = X(z,t)$ as a function of depth z and time t [9]. This PDE is based on the solid and liquid mass balances, and its coefficients depend discontinuously on z.

Important applications also involve chemical reactions between different components of the solid and liquid phases. An example in wastewater treatment are biokinetic reactions between flocculated activated sludge (bacteria) and substrates (nutrients) dissolved in the liquid. This work extends the model of continuous sedimentation with compression to such combined processes by including the transport and reaction of these components. The final model can be written as the system of PDEs

$$\partial_t X + \partial_z\big(\mathcal{F}(X,z,t) - \gamma(z)\partial_z D(X)\big) = \mathcal{A}_X(X,\boldsymbol{p}_X,\bar{\boldsymbol{p}}_L,z,t), \tag{1a}$$

$$\partial_t(\boldsymbol{p}_X X) + \partial_z\big(\boldsymbol{p}_X\big(\mathcal{F}(X,z,t) - \gamma(z)\partial_z D(X)\big)\big) = \boldsymbol{\mathcal{A}}_X(X,\boldsymbol{p}_X,\bar{\boldsymbol{p}}_L,z,t), \tag{1b}$$

$$\partial_t(\bar{\boldsymbol{p}}_L l_1(X)) + \partial_z\big(\bar{\boldsymbol{p}}_L l_2\big(\mathcal{F}(X,z,t) - \gamma(z)\partial_z D(X),z,t\big)\big) = \boldsymbol{\mathcal{A}}_L(X,\boldsymbol{p}_X,\bar{\boldsymbol{p}}_L,z,t) \tag{1c}$$

*This work is supported was funded by CONICYT (Chile) through projects Fondecyt 1130154; BASAL project CMM, Universidad de Chile and Centro de Investigación en Ingeniería Matemática (CI^{2}MA), Universidad de Concepción; Anillo ACT1118 (ANANUM); CRHIAM, project CONICYT/FONDAP/15130015; and Fondef ID15I10291 (to R.B.) and CONICYT scholarship (to C.M.).

†CI^{2}MA and Departamento de Ingeniería Matemática, Facultad de Ciencias Físicas y Matemáticas, Universidad de Concepción, Casilla 160-C, Concepción, Chile (rburger@ing-mat.udec.cl), (cmejias@ing-mat.udec.cl)

‡Centre for Mathematical Sciences, Lund University, P.O. Box 118, S-221 00 Lund, Sweden (diehl@maths.lth.se) (corresponding author), submitted June 14, 2016

for $z \in \mathbb{R}$ and $t > 0$, along with suitable initial conditions. The convective flux function $\mathcal{F}$ describes the bulk flow and hindered settling, while the function D accounts for sediment compressibility. The characteristic function $\gamma(z) = 1$ if $-H < z < B$, i.e. inside the settling tank, and $\gamma(z) = 0$ outside; see Figure 1 (a). Both $\mathcal{F}$ and D depend nonlinearly on X and discontinuously on z, and it is assumed that $D = 0$ on an X-interval of positive length, so the model is strongly degenerate and its solutions will, in general, be discontinuous. Moreover, $\boldsymbol{p}_X = \boldsymbol{p}_X(z,t)$ and $\bar{\boldsymbol{p}}_L = \bar{\boldsymbol{p}}_L(z,t)$ are vectors of unknown (mass) percentages of components of the solid particles and the fluid, l_1 and l_2 are certain given functions, and $\mathcal{A}_X$, $\boldsymbol{\mathcal{A}}_X$ and $\boldsymbol{\mathcal{A}}_L$ are algebraic functions of their arguments and stand for given feed and reaction terms. (Precise definitions and assumptions are provided in later parts of the paper.)

We herein derive the new model (1) from volume, mass, and chemical balances and suitable constitutive assumptions, and focus on its numerical solution. The main novelty is a difference scheme that combines the approach of [5, 9] for the non-reactive case (i.e., suitable for (1a) in the absence of reactions) with the numerical percentage transport introduced in [14] for a related multi-component, non-reactive model. The main mathematical result is an invariant region principle for the numerical scheme proved under a suitable CFL condition. This result ensures that numerical solutions are physically relevant and, in particular, non-negative. Two examples illustrate the predictions of the new model and the convergence property of the scheme.

1.2. Related work. For the non-reactive case, the first model was analyzed in [12] for the hyperbolic case ($D \equiv 0$), modelling hindered settling, and was extended in [9] with a strongly degenerate diffusion function $D \not\equiv 0$ to model compression at high solids concentrations. References to further extensions such as vessels with varying cross-sectional area and polydisperse suspensions, as well as other applications leading to an equation of type (1a), include [7, 10, 15, 21].

The discontinuous dependence of $\mathcal{F}$ on z and the presence of $\gamma(z)$ come from the modelling of the inlet and outlet streams of the sedimentation tank. Therefore, in the non-reactive case, (1a) represents an application of the theory of first-order conservation laws with discontinuous flux and its extensions to degenerate parabolic equations. It is well known that solutions of such equations are in general discontinuous and need to be defined as weak solutions along with a selection criterion or entropy condition to ensure uniqueness. Thus the main mathematical issues posed by (1a) were to find suitable uniqueness conditions and establish well-posedness, given the difficulty of the discontinuous dependence of $\mathcal{F}$ and γ on z (in addition to the nonlinear dependence of $\mathcal{F}$ on X) [9, 11, 13, 16, 17, 21], as well as to define numerical schemes that provably converge to the unique solution [8]. The well-posedness and numerical analysis of [9] is strongly based on the work by Karlsen, Risebro, and Towers [26, 27, 28].

The well-posedness and numerical analysis of equations of the non-reactive version of (1a) has led to a recent simulation model for secondary settling tanks (SSTs) in wastewater treatment and an adhering numerical scheme [5, 6]. That model has shown to give more realistic predictions [29, 35] than previous state-of-the-art models.

There are several motivations for extending our previous non-reactive model to the system (1). In both mineral processing and wastewater treatment, liquid flocculant added to the suspension sticks to the small particles so that larger flocs are formed and thereby their settling velocity increased. The importance of modelling reactive sedimentation in wastewater treatment has been demonstrated by different approaches [1, 19, 20, 23, 24, 30, 31]. Similar phenomena modelled with PDEs are flocculation in mineral processing [33], multi-component two-phase flow in porous media [2, 3]

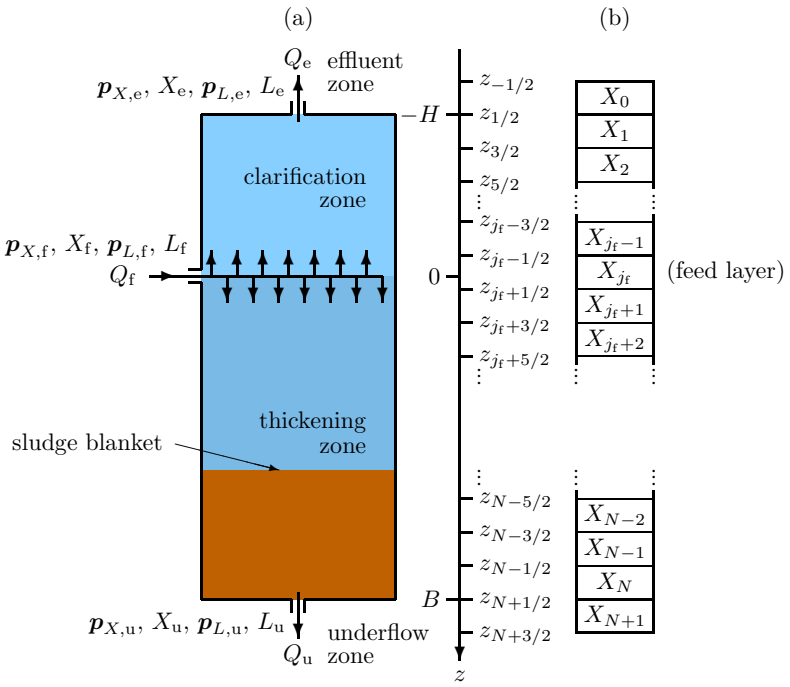

FIG. 1. *(a) An ideal secondary settling tank (SST) with variables of the feed inlet, effluent and underflow corresponding to the indices* f, e *and* u, *respectively. The effluent, clarification, thickening, and underflow zones correspond to the respective intervals* $z < -H$, $-H < z < 0$, $0 < z < B$, *and* $z > B$. *The sludge blanket (concentration discontinuity) separates the hindered settling zone and the compression zone. (b) Aligned illustration of the subdivision of the SST into layers (see Section 3).*

and particle-size segregation in granular avalanches [22]. Another application with potential modelling advantages is counter-current "washing" of solids, a process in hydrometallurgy where a soluble constituent is extracted from a solid by means of a solvent. This is achieved by coupling a series of clarifier-thickeners [32, 34].

A PDE model and numerical scheme for batch sedimentation (closed vessel) of two particulate components including a reduced biokinetic model in wastewater treatment were presented in [4]. The movements of the substrates were only modelled by a simple diffusion coefficient. For the numerical examples presented herein for continuous sedimentation we use the same biokinetic denitrification reactions as in [4].

From the viewpoint of scientific computing it is a known problem that standard fluxes for finite volume schemes do not preserve the fundamental requirements that the mass percentages belong to the interval $[0, 1]$ and their sum is always equal to one [25]. This is handled by our numerical scheme.

1.3. Outline of the remainder of the paper. In Section 2, the model is derived. To this end, we introduce in Section 2.1 the concept of an ideal secondary settling tank (SST) (see Figure 1), the model variables and some fundamental assumptions. Simplifying assumptions typical of wastewater treatment are collected in Section 2.2. The mathematical model, based on conservation laws, are stated in Section 2.3. To convert these equations into an equivalent model suitable for simulation, we first replace (in Section 2.4) the abstract solid and fluid phase velocities by a mixture bulk velocity, expressed by the given volumetric flows and model variables, and a

solid-fluid relative velocity, prescribed by constitutive functions. Next, in Section 2.5 we derive explicit expressions for the total fluxes of the solid and liquid phases, and after further reformulations arrive in Section 2.6 at the mathematical model in final, solvable form akin to (1). To close the model we introduce in Section 2.7 constitutive functions for hindered and compressive settling, and address in Section 2.8 the choice of initial data and feed input functions. Next, in Section 3, a numerical scheme for the model is developed. This is done via a method-of-lines discretization (Section 3.1) that combines ingredients from [5] and [14]. A time discretization leading to a fully discrete scheme is introduced in Section 3.2, and the corresponding CFL condition is stated in Section 3.3. Section 4 is devoted to the proof, via several lemmas that appeal to monotonicity arguments, of the main mathematical result, Theorem 2, which states that the scheme satisfies an invariant region principle. In Section 5, we present two numerical examples for a model of denitrification in wastewater treatment. Two examples illustrate the response of the SST to variations of either the feed flow or the feed percentages. Based on these, Section 5.4 contains estimations of error and convergence order. Concluding remarks are offered in Section 6.

2. Model formulation.

2.1. Assumptions. In mineral processing and hyrometallurgy, continuously operated sedimentation tanks are usually referred to as "clarifier-thickeners" or simply "thickeners", and in wastewater treatment (our main motivation) as "secondary clarifiers" or "secondary settling tanks" (SSTs). The ideal SST shown in Figure 1 (a) has a constant cross-sectional area A. The concentration of each component is assumed to depend only on time t and depth z measured from the feed inlet located at $z = 0$. The balance laws that make up the model hold for $z \in \mathbb{R}$, have coefficients that are spatially discontinuous at $z = -H$, 0 and B, and need no boundary conditions. The suspension is constituted by the solid phase that consists of particles and the liquid phase that consists of substrates dissolved in water.

The total concentration of particles (or the solid phase) is denoted by $X(z,t)$. Each (flocculated) particle is assumed to consist of a number k_X of components described by the (mass) percentage vector

$$\boldsymbol{p}_X = \left(p_X^{(1)}, p_X^{(2)}, \ldots, p_X^{(k_X)}\right)^{\mathrm{T}}, \quad \text{where } p_X^{(1)} + \cdots + p_X^{(k_X)} = 1. \tag{2}$$

The effluent concentration is $X_{\mathrm{e}}(t) := \lim_{\varepsilon \to 0^+} X(-H - \varepsilon, t)$. The underflow concentration X_{u} and the percentage vectors $\boldsymbol{p}_{X,\mathrm{e}}$ and $\boldsymbol{p}_{X,\mathrm{u}}$ are defined analogously. The concentrations of all solid components are $\boldsymbol{p}_X X =: \boldsymbol{C} = (C^{(1)}, \ldots, C^{(k_L)})^{\mathrm{T}}$. For $X = 0$ the values of $\boldsymbol{p}_X$ are irrelevant; however, they should always satisfy (2).

The total concentration of the liquid phase is denoted by $L(z,t)$. The percentage vector $\boldsymbol{p}_L$ and the concentrations at the outlets are defined in the same way as for the particulate phase. We assign the last percentage $p_L^{(k_L)}$ for the water component, which is much larger than the percentages of the soluble components $p_L^{(i)}$, $i = 1, \ldots, k_L - 1$. If the concentrations of the soluble components are contained in the vector $\boldsymbol{S} = (S^{(1)}, \ldots, S^{(k_L-1)})^{\mathrm{T}}$ and W denotes the water component, then

$$\boldsymbol{p}_L L = \begin{pmatrix} \boldsymbol{S} \\ W \end{pmatrix}, \quad \text{where} \quad W = p_L^{(k_L)} L = \left(1 - \sum_{i=1}^{k_L-1} p_L^{(i)}\right) L = L - \sum_{i=1}^{k_L-1} S^{(i)}. \tag{3}$$

The concentrations X_{f}, L_{f}, percentage vectors $\boldsymbol{p}_{X,\mathrm{f}}$, $\boldsymbol{p}_{L,\mathrm{f}}$, and volumetric flows $Q_{\mathrm{f}} \geq Q_{\mathrm{u}} > 0$ are given functions of time. It turns out that the effluent volumetric

flow $Q_{\mathrm{e}}(t;\boldsymbol{C},\boldsymbol{S})$ generally depends on unknown variables via the reaction terms; see Section 2.4. We define $q_{\mathrm{f}} := Q_{\mathrm{f}}/A$, $q_{\mathrm{e}} := Q_{\mathrm{e}}/A$ and $q_{\mathrm{u}} := Q_{\mathrm{f}}/A$.

The density of the solid phase ρ_X is assumed to be constant and much greater than the maximum packing concentration of the solids X_{m}.

The (unknown) solid and liquid phase velocities are denoted by $v_X = v_X(z,t)$ and $v_L = v_L(z,t)$, respectively. Inside the SST, the particles undergo hindered settling and compression according to some constitutive function for the relative velocity

$$v_X - v_L =: v_{\mathrm{rel}} = v_{\mathrm{rel}}(X, \partial_z X) \qquad \text{(see Section 2.7)}. \tag{4}$$

In the effluent and underflow zones, both phases move at the same velocity, i.e.,

$$v_{\mathrm{rel}} := 0 \quad \text{for } z < -H \text{ and } z \geq B. \tag{5}$$

The reaction terms for all particulate and soluble components are collected in the vectors $\boldsymbol{R}_X(\boldsymbol{C},\boldsymbol{S})$ of length k_X and $\boldsymbol{R}_L(\boldsymbol{C},\boldsymbol{S})$ of length k_L. We define

$$\tilde{R}_X(\boldsymbol{C},\boldsymbol{S}) := \sum_{i=1}^{k_X} R_X^{(i)}(\boldsymbol{C},\boldsymbol{S}), \quad \tilde{R}_L(\boldsymbol{C},\boldsymbol{S}) := \sum_{i=1}^{k_L} R_L^{(i)}(\boldsymbol{C},\boldsymbol{S}).$$

We assume that every volume of the suspension initially contains either of the two phases in the SST and always for the feed input. For a small volume $V = V_X + V_L$ of suspension, where V_X and V_L are the respective volume of each phase, the masses of the two phases in V can be expressed as $\rho_X V_X = XV$ and $\rho_L v_L = LV$, respectively.

REMARK 1. *To allow for defining local values of density, concentration and volume fraction, the volume V should be sufficiently small but contain enough particles to be representative. We refer to [18] for a discussion including different definitions involving, e.g., the average or expected values of V_X and the mass m_X such that the limit $\lim_{V\to 0^+} m_X/V_x$ exists and can define the density ρ_X.*

2.2. Specific assumptions for wastewater treatment. The assumptions stated so far refer to continuous sedimentation with reactions in any application. The further analysis of the model and the numerical scheme will, however, rely on some simplifying assumptions typical of wastewater treatment and biological reactions.

We denote the densities of the liquid components by $\rho_L^{(i)}$, $i = 1,\dots,k_L$. Since the liquid phase from a biological reactor consists almost entirely of water, i.e., $p_L^{(i)} \ll p_L^{(k_L)} \approx 1$ for $i \neq k_L$, the average density of the liquid phase ρ_L satisfies

$$\rho_L = p_L^{(1)}\rho_L^{(1)} + \cdots + p_L^{(k_L)}\rho_L^{(k_L)} \approx \rho_L^{(k_L)}. \tag{6}$$

Thus, the density of the liquid phase ρ_L is assumed to be constant.

The water concentration $W = p_L^{(k_L)} L$ does not influence any reaction, and is not influenced by any reaction, so that $R_L^{(k_L)} = 0$. We assume zero growth of bacteria when there is no, i.e., $\boldsymbol{R}_{X,j}(\boldsymbol{0},\boldsymbol{S}) = \boldsymbol{0}$, and allow that the soluble substrate concentration may increase due to decay of bacteria, that is, $\boldsymbol{R}_{L,j}(\boldsymbol{C},\boldsymbol{0}) \geq 0$. Furthermore, we assume that there are no reaction in the effluent and underflow regions. Moreover, the following assumptions are technical but not restrictive for the application:

$$\tilde{R}_X(\boldsymbol{p}_X X_{\mathrm{m}}, \boldsymbol{S}) = 0, \qquad v_{\mathrm{rel}}(X_{\mathrm{m}}, \partial_z X) = 0. \tag{7}$$

The former states that the bacteria cannot grow when they have reached the maximum concentration X_{m} and the latter that the particles follow the liquid flow at X_{m}.

The term of $Q_{\mathrm{e}}(t;\boldsymbol{C},\boldsymbol{S})$ that depends on $\boldsymbol{C}$ and $\boldsymbol{S}$ (see Section 2.4) seems to be negligible in wastewater treatment and setting this to zero, we partly have the standard relation $Q_{\mathrm{f}}(t) = Q_{\mathrm{u}}(t) + Q_{\mathrm{e}}(t)$, and partly can prove Theorem 2.

2.3. Mass balance equations. The fundamental equation that every volume of the suspension contains either of the two phases can be written as

$$V_X + V_L = V \quad \Leftrightarrow \quad \frac{X}{\rho_X} + \frac{L}{\rho_L} = 1 \quad \Leftrightarrow \quad L = \rho_L - rX, \quad \text{where } r := \frac{\rho_L}{\rho_X}. \tag{8}$$

We assume that this is satisfied for the given feed concentrations; $X_\mathrm{f}/\rho_X + L_\mathrm{f}/\rho_L = 1$. The assumption $\rho_X > X_\mathrm{m}$ implies that always $L > 0$.

The conservation of mass for each particulate and soluble/liquid component and the requirements of the percentages imply the following system of equations for $z \in \mathbb{R}$ and $t > 0$, where $\delta(z)$ is the delta function:

$$\partial_t(\boldsymbol{p}_X X) + \partial_z(\boldsymbol{p}_X X v_X) = \delta(z)\boldsymbol{p}_{X,\mathrm{f}} X_\mathrm{f} q_\mathrm{f} + \gamma(z)\boldsymbol{R}_X(\boldsymbol{C}, \boldsymbol{S}), \tag{9a}$$

$$\partial_t(\boldsymbol{p}_L L) + \partial_z(\boldsymbol{p}_L L v_L) = \delta(z)\boldsymbol{p}_{L,\mathrm{f}} L_\mathrm{f} q_\mathrm{f} + \gamma(z)\boldsymbol{R}_L(\boldsymbol{C}, \boldsymbol{S}), \tag{9b}$$

$$p_X^{(1)} + \cdots + p_X^{(k_X)} = 1, \tag{9c}$$

$$p_L^{(1)} + \cdots + p_L^{(k_L)} = 1. \tag{9d}$$

2.4. Phase, bulk, and relative velocities. The full set of $k_X + k_L + 4$ balance equations are (4), (8) and (9) and the unknowns are $\boldsymbol{p}_X$, X, $\boldsymbol{p}_L$, L, v_X and v_L. We now reduce the number of equations by eliminating the variables v_X and v_L. This will be achieved by first replacing them with v_rel and the average bulk velocity of the suspension q, and then expressing q in terms of the rest of the unknowns.

LEMMA 1. *Equations* (9a) *and* (9c) *are equivalent to* (9a) *and*

$$\partial_t X + \partial_z(X v_X) = \delta(z) X_\mathrm{f} q_\mathrm{f} + \gamma(z)\tilde{R}_X. \tag{10}$$

Analogously, (9b) *and* (9d) *are equivalent to* (9b) *and*

$$\partial_t L + \partial_z(L v_L) = \delta(z) L_\mathrm{f} q_\mathrm{f} + \gamma(z)\tilde{R}_L. \tag{11}$$

Proof. Summing all equations in (9a), using (9c) and that $\boldsymbol{p}_{X,\mathrm{f}}$ satisfies (2), we get (10). Conversely, summing all equations in (9a) and subtracting (10) implies (9c). ∎

With the volume fraction of the solid phase $\phi := V_X/V$, we have $X = \rho_X \phi$ and $L = \rho_L(1-\phi)$, cf. (8). Analogously, the feed inlet concentrations can be written as $X_\mathrm{f} = \rho_X \phi_\mathrm{f}$ and $L_\mathrm{f} = \rho_L(1-\phi_\mathrm{f})$. Substituting these expressions into (10) and (11) and dividing by the constant densities ρ_X and ρ_L, respectively, we get

$$\begin{aligned} \partial_t \phi + \partial_z(\phi v_X) &= \delta(z)\phi_\mathrm{f} q_\mathrm{f} + \gamma(z)\tilde{R}_X \rho_X^{-1}, \\ \partial_t(1-\phi) + \partial_z\big((1-\phi)v_L\big) &= \delta(z)(1-\phi_\mathrm{f}) q_\mathrm{f} + \gamma(z)\tilde{R}_L \rho_L^{-1}. \end{aligned}$$

Adding these two equations and defining

$$q(z,t) := \phi v_X(z,t) + (1-\phi) v_L(z,t) \quad \text{(average bulk velocity)}, \tag{12}$$

$$\mathcal{R}(\boldsymbol{C}, \boldsymbol{S}) := \tilde{R}_X(\boldsymbol{C}, \boldsymbol{S})\rho_X^{-1} + \tilde{R}_L(\boldsymbol{C}, \boldsymbol{S})\rho_L^{-1}, \tag{13}$$

we get an equation without any time derivative:

$$\partial_z q = \delta(z) q_\mathrm{f} + \gamma(z)\mathcal{R}(\boldsymbol{C}, \boldsymbol{S}). \tag{14}$$

We can express v_X and v_L in terms of q and v_{rel} since (4) and (12) are equivalent to $v_X = q + v$ and $v_L = q - \phi v_{\mathrm{rel}}$ with the batch settling velocity $v := (1-\phi)v_{\mathrm{rel}}$. We now derive an explicit expression for q. In view of (5), (12) implies:

$$q(z,t) = \begin{cases} v_X(z,t) = v_L(z,t) = -q_{\mathrm{e}}(t) & \text{for } z \le -H, \\ v_X(z,t) = v_L(z,t) = q_{\mathrm{u}}(t) & \text{for } z \ge B, \end{cases} \tag{15}$$

where q_{u} is known and q_{e} is unknown. We integrate (14) from z to B to get

$$q(z,t;\boldsymbol{C},\boldsymbol{S}) = q(B,t) - \int_z^B \Big(\delta(\xi) q_{\mathrm{f}}(t) + \gamma(\xi)\mathcal{R}\big(\boldsymbol{C}(\xi,t),\boldsymbol{S}(\xi,t)\big)\Big)\,\mathrm{d}\xi. \tag{16}$$

The following function describes the additional bulk velocity due to the reactions:

$$q^{\mathrm{reac}}(z;\boldsymbol{C},\boldsymbol{S}) := \int_z^B \gamma(\xi)\mathcal{R}(\boldsymbol{C},\boldsymbol{S})\,\mathrm{d}\xi. \tag{17}$$

Since by (15), $q(B,t) = q_{\mathrm{u}}(t)$, we may express q in terms of the unknowns as follows:

$$q(z,t;\boldsymbol{C},\boldsymbol{S}) := \begin{cases} q_{\mathrm{u}}(t) - q_{\mathrm{f}}(t) - q^{\mathrm{reac}}(-H;\boldsymbol{C},\boldsymbol{S}) & \text{for } z \le -H, \\ q_{\mathrm{u}}(t) - q_{\mathrm{f}}(t) - q^{\mathrm{reac}}(z;\boldsymbol{C},\boldsymbol{S}) & \text{for } -H < z < 0, \\ q_{\mathrm{u}}(t) - q^{\mathrm{reac}}(z;\boldsymbol{C},\boldsymbol{S}) & \text{for } 0 < z < B, \\ q_{\mathrm{u}}(t) & \text{for } z \ge B. \end{cases} \tag{18}$$

Moreover, (15) states that $q(z,t) = -q_{\mathrm{e}}(t)$ for $z \le -H$, so (18) defines the effluent bulk velocity in terms of the unknowns: $q_{\mathrm{e}}(t;\boldsymbol{C},\boldsymbol{S}) = q_{\mathrm{f}}(t) - q_{\mathrm{u}}(t) + q^{\mathrm{reac}}(-H;\boldsymbol{C},\boldsymbol{S})$.

2.5. Solid and liquid total fluxes. The flux functions of the PDEs (10) for X and (11) for L can be written as

$$Xv_X = Xq + Xv, \tag{19}$$

$$Lv_L = \rho_L(1-\phi)(q - \phi v_{\mathrm{rel}}) = \rho_L\big((1-\phi)q - \phi v\big) = \rho_L\left(q - (Xq + Xv)\rho_X^{-1}\right). \tag{20}$$

Thus, we define the total fluxes in terms of q and $v = (1-\phi)v_{\mathrm{rel}}$ as follows:

$$F_X := Xq + Xv = Xq + X(1 - X\rho_X^{-1})v_{\mathrm{rel}}, \tag{21}$$

$$F_L := \rho_L q - rF_X \quad \Leftrightarrow \quad F_X\rho_X^{-1} + F_L\rho_L^{-1} = q. \tag{22}$$

With q defined by (18), F_X by (21) and F_L by (22) we get the following governing equations, which neither contain v_X nor v_L:

$$\partial_t(\boldsymbol{p}_X X) + \partial_z(\boldsymbol{p}_X F_X) = \delta(z)\boldsymbol{p}_{X,\mathrm{f}} X_{\mathrm{f}} q_{\mathrm{f}} + \gamma(z)\boldsymbol{R}_X(\boldsymbol{C},\boldsymbol{S}), \tag{23a}$$

$$\partial_t(\boldsymbol{p}_L L) + \partial_z(\boldsymbol{p}_L F_L) = \delta(z)\boldsymbol{p}_{L,\mathrm{f}} L_{\mathrm{f}} q_{\mathrm{f}} + \gamma(z)\boldsymbol{R}_L(\boldsymbol{C},\boldsymbol{S}), \tag{23b}$$

$$p_X^{(1)} + \cdots + p_X^{(k_X)} = 1, \tag{23c}$$

$$p_L^{(1)} + \cdots + p_L^{(k_L)} = 1. \tag{23d}$$

The proof of the following lemma is analogous to that of Lemma 1.

LEMMA 2. *Equations* (23a) *and* (23c) *are equivalent to* (23a) *and*

$$\partial_t X + \partial_z F_X = \delta(z) X_{\mathrm{f}} q_{\mathrm{f}} + \gamma(z)\tilde{R}_X. \tag{24}$$

Analogously, (23b) *and* (23d) *are equivalent to* (23b) *and*

$$\partial_t L + \partial_z F_L = \delta(z) L_{\mathrm{f}} q_{\mathrm{f}} + \gamma(z)\tilde{R}_L. \tag{25}$$

LEMMA 3. *Equations* (24) *and* (25) *are equivalent to* (24) *and* (8).

Proof. Dividing (24) by ρ_X, (25) by ρ_L and summing these two equations, we get the following equation which can replace (25) (with maintained equivalence):

$$\frac{\partial}{\partial t}\left(\frac{X}{\rho_X}+\frac{L}{\rho_L}\right)+\frac{\partial}{\partial z}\left(\frac{F_X}{\rho_X}+\frac{F_L}{\rho_L}\right)=\delta(z)q_{\mathrm{f}}\left(\frac{X_{\mathrm{f}}}{\rho_X}+\frac{L_{\mathrm{f}}}{\rho_L}\right)+\gamma(z)\left(\frac{\tilde{R}_X}{\rho_X}+\frac{\tilde{R}_L}{\rho_L}\right)$$

All terms except the first cancel out. This is because of the equality (22), the expression (16) for q and the definition of $\mathcal{R}$ in (13). The remaining equation is

$$\frac{\partial}{\partial t}\left(\frac{X}{\rho_X}+\frac{L}{\rho_L}\right)=0 \quad\Longleftrightarrow\quad \frac{\partial}{\partial t}\left(\frac{V_X}{V}+\frac{V_L}{V}\right)=0 \quad\Longleftrightarrow\quad \frac{V_X}{V}+\frac{V_L}{V}=g(z),$$

where the function $g(z)$ must be equal to one, since it is at time $t=0$ by assumption. Hence, the remaining equations is equivalent to (8). ∎

LEMMA 4. *Equations* (4) *and* (9) *are equivalent to the governing equations* (23).

Proof. Given (4)–(9d), Lemma 1 states that (9c) and (9d) can be replaced (keeping the equivalence) by (10) and (11). Equations (4)–(8) imply via (19)–(22) that $Xv_x = F_X$ and $Lv_L = F_L$. Hence, (10) and (11) are equivalent to (24) and (25), which by Lemma 2 can be replaced by (23c) and (23d). For the other implication, we should prove that (4), (8), $F_X = Xv_X$ and $F_L = Lv_L$ hold. Lemma 2 implies first that (23c) and (23d) can be replaced by (24) and (25). Then Lemma 3 implies (8). Since $v_X = q + v$ and $v_L = q - \phi v_{\mathrm{rel}}$, (4) is directly satisfied and $F_X = X(q+v) = Xv_X$. With this equality and $\phi = X/\rho_X$, we obtain from (12) $F_X/\rho_X + (1 - X/\rho_X)v_L = q$. Substituting this into the definition of F_L (22), we get $F_L = \rho_L(q - rF_X) = (\rho_L - rX)v_L = Lv_L$, where the last equality follows from (8). ∎

2.6. Model equations in final form. Finally, we observe that the last scalar equation of (23b) determines $p_L^{(k_L)}$ for the water component of the liquid. This variable does not appear in any other equation. A simpler equation to determine $p_L^{(k_L)}$ is (23d). Let the notation with a bar $\bar{\boldsymbol{p}}_L$ denote the first $k_L - 1$ components of $\boldsymbol{p}_L$.

THEOREM 1. *The balance equations* (4) *and* (9) *are equivalent to the following set of model equations defined for* $z \in \mathbb{R}$ *and* $t > 0$*:*

$$\partial_t X + \partial_z F_X = \delta(z)X_{\mathrm{f}}q_{\mathrm{f}} + \gamma(z)\tilde{R}_X, \tag{26a}$$

$$\partial_t(\boldsymbol{p}_X X) + \partial_z(\boldsymbol{p}_X F_X) = \delta(z)\boldsymbol{p}_{X,\mathrm{f}}X_{\mathrm{f}}q_{\mathrm{f}} + \gamma(z)\boldsymbol{R}_X, \tag{26b}$$

$$L = \rho_L - rX, \tag{26c}$$

$$\partial_t(\bar{\boldsymbol{p}}_L L) + \partial_z(\bar{\boldsymbol{p}}_L F_L) = \delta(z)\bar{\boldsymbol{p}}_{L,\mathrm{f}}L_{\mathrm{f}}q_{\mathrm{f}} + \gamma(z)\bar{\boldsymbol{R}}_L, \quad \text{where } F_L = \rho_L q - rF_X, \tag{26d}$$

$$p_L^{(k_L)} = 1 - \big(p_L^{(1)} + \cdots + p_L^{(k_L-1)}\big). \tag{26e}$$

Proof. We apply Lemmas 4, 2 and 3 (in that order) to obtain equivalently (26a)–(26c) and (23b). It remains to prove that (23b) can be split into (26d) and (26e). Lemma 3 states that we can replace (26c) by (25), which in turn by Lemma 2 can be replaced by (26e). Conversely, summing the equations in (26d), recalling that $R_L^{(k_L)} = 0$ and using (26e), we get

$$\partial_t\big((1 - p_L^{(k_L)})L\big) + \partial_z\big((1 - p_L^{(k_L)})F_L\big) = \delta(z)(1 - p_{L,\mathrm{f}}^{(k_L)})L_{\mathrm{f}}q_{\mathrm{f}} + \gamma(z)\tilde{R}_L$$

Now subtract (25) to obtain the last equation of (23b). ∎

The specific advantages of the order and form of Equations (26) are the following. Firstly, for a numerical method, with explicit or implicit time stepping, the value of X at the new time point is obtained by solving (26a) only. Then the vector $\boldsymbol{p}_X$ is updated by (26b), etc. Secondly, this form of the governing equations yield the invariant-region property of the numerical scheme (see Section 4).

2.7. Constitutive functions for hindered and compressive settling. Consistently with [4, 6, 9] we assume that v or equivalently, $v_{\mathrm{rel}} = v/(1-\phi)$, is given by

$$v = v(X, \partial_z X, z) = \gamma(z) v_{\mathrm{hs}}(X) \left(1 - \frac{\rho_X \sigma_{\mathrm{e}}'(X)}{X g(\rho_X - \rho_L)} \partial_z X\right).$$

Here, v_{hs} is the hindered settling velocity function and σ_{e} the effective solids stress. Constitutive functions are needed for v_{hs} and σ_{e}; see Section 5. We require that $\sigma_{\mathrm{e}}(X) = 0$ for $X < X_{\mathrm{c}}$, where X_{c} is a critical concentration above which the particles form a network, and $\sigma_{\mathrm{e}}'(X) \geq 0$ for $X > X_{\mathrm{c}}$ (see [9]). It is convenient to define

$$f_{\mathrm{b}}(X) := X v_{\mathrm{hs}}(X), \quad d(X) := v_{\mathrm{hs}}(X) \frac{\rho_X \sigma_{\mathrm{e}}'(X)}{g(\rho_X - \rho_L)}, \quad D(X) := \int_{X_{\mathrm{c}}}^{X} d(s)\,\mathrm{d}s. \tag{27}$$

With the batch settling flux function $f_{\mathrm{b}}(X)$, the total particulate flux (21) becomes

$$F_X(X, \partial_z X, z, t) = X q(z,t) + \gamma(z)\big(f_{\mathrm{b}}(X) - \partial_z D(X)\big). \tag{28}$$

Remark 2. *We verify that the final model can be expressed as (1) when the reactive bulk velocity is neglected, i.e., $q^{\mathrm{reac}} := 0$. Then (18) implies that $q = q(z,t)$, and comparing (1a) with (26a) and (28), we get $\mathcal{F}(X,z,t) = Xq(z,t) + \gamma(z) f_{\mathrm{b}}(X)$. Moreover, by (8) we can express $L = l_1(X) := \rho_L - rX$. Thus, all variables $\boldsymbol{p}_X$, X, $\boldsymbol{p}_L$, L, $\boldsymbol{S}$ and $\boldsymbol{C}$ can be expressed in terms of $\boldsymbol{p}_X$, $\bar{\boldsymbol{p}}_L$ and X, so that that the right-hand sides of (26a), (26b) and (26d) can be written as functions $\boldsymbol{\mathcal{A}}_X$, $\boldsymbol{\mathcal{A}}_X$ and $\boldsymbol{\mathcal{A}}_L$, respectively, of $(X, \boldsymbol{p}_X, \bar{\boldsymbol{p}}_X, z, t)$. Finally, (22) gives $F_L = l_2(F_X, z, t) := \rho_L q(z,t) - r F_X$.*

2.8. Initial data and feed input functions. Initial data at $t = 0$, namely

$$X(z,0) = X^0(z), \quad \boldsymbol{p}_X(z,0) = \boldsymbol{p}_X^0(z), \quad \boldsymbol{p}_L(z,0) = \boldsymbol{p}_L^0(z), \quad L(z,0) = L^0(z), \quad z \in \mathbb{R}$$

are obtained either from direct information on the particulate total concentration $X^0(z)$ and the percentage vector $\boldsymbol{p}_X^0(z)$, or from given concentrations of all components: $\boldsymbol{p}_X^0 X^0 = \boldsymbol{C}^0 = (C^{(1),0}, \ldots, C^{(k_X),0})^{\mathrm{T}}$. In the latter case, summation yields

$$X^0 = X^0\big(p_X^{(1),0} + \cdots + p_X^{(k_X),0}\big) = C^{(1),0} + \cdots + C^{(k_X),0} \quad \text{and} \quad \boldsymbol{p}_X^0 = \boldsymbol{C}^0 / X^0.$$

If $\boldsymbol{S}^0 = (S^{(1),0}, S^{(2),0}, \ldots, S^{(k_L-1),0})^{\mathrm{T}}$ denotes the concentrations of the initial soluble components, then (8) and (3) give $L^0 = \rho_L - rX^0$ and

$$\boldsymbol{p}_L^0 = \begin{pmatrix} \boldsymbol{S}^0 / L^0 \\ 1 - \sum_{i=1}^{k_L - 1} S^{(i),0} / L^0 \end{pmatrix}.$$

The feed input functions $\boldsymbol{p}_{X,\mathrm{f}}(t)$, $X_{\mathrm{f}}(t)$, $\boldsymbol{p}_{L,\mathrm{f}}(t)$ and $L_{\mathrm{f}}(t)$ are defined analogously.

3. Numerical scheme. As in [5], we divide the SST into N internal computational cells, or layers, of depth $\Delta z = (B+H)/N$; see Figure 1 (b). The midpoint of layer j is assumed to have the coordinate z_j, hence the layer is the interval $[z_{j-1/2}, z_{j+1/2}]$. Layer 1, the top layer in the clarification zone, is thus

$[z_{1/2}, z_{3/2}] = [-H, -H + \Delta z]$, and the bottom location is $z = z_{N+1/2} = B$. We define j_f to be the smallest integer larger than or equal to $H/\Delta z$, i.e., $j_\mathrm{f} := \lceil H/\Delta z \rceil$. Then the feed inlet ($z = 0$) is located in layer j_f (the feed layer). Layers -1 and $N+1$ have been added to obtain the correct effluent and underflow concentrations, respectively. The average values of the unknowns in each layer j are denoted by $\boldsymbol{P}_{X,j} = \boldsymbol{P}_{X,j}(t)$, $X_j = X_j(t)$, etc. The unknown output functions at the effluent and underflow are $X_\mathrm{e}(t) := X_0(t)$, $X_\mathrm{u}(t) := X_{N+1}(t)$, etc. To simplify formulas below, we use two mirror cells and set $X_{-1} := X_0$, $X_{N+2} := X_{N+1}$ and analogously for other variables.

3.1. Spatial discretization. The computational domain is composed of $N+2$ intervals and one needs to define numerical fluxes for $N+3$ layer boundaries. Except for the reaction term, (26a) is a model for which a working numerical scheme is available [5]. The reaction term depends on all variables, and is strongly coupled to the other equations via the total flux (21), which contains the bulk velocity $q = q(z, t, \boldsymbol{C}, \boldsymbol{S})$, which, in contrast to the non-reactive case, depends on the unknown concentrations via q^reac in (17), (18). This function is well defined at $z_{j+1/2}$, because of the integration in (17). For piecewise constant functions in each layer, i.e. $X(z,t) = X_j$, $z \in (z_{j-1/2}, z_{j+1/2}]$, etc., we obtain (recall that $\mathcal{R} = 0$ outside the SST)

$$q^\mathrm{reac}_{j+1/2} := q^\mathrm{reac}(z_{j+1/2}) := \begin{cases} \sum_{i=j+1}^{N} \gamma_i \mathcal{R}_i \Delta z & \text{for } j = -1, \dots, N-1, \\ 0 & \text{for } j = N, N+1, \end{cases} \tag{29}$$

and then define $q_{j+1/2} := q(z_{j+1/2}, t)$ in accordance with (18):

$$q_{j+1/2} = \begin{cases} q_\mathrm{u}(t) - q_\mathrm{f}(t) - \sum_{i=j+1}^{N} \mathcal{R}_i \Delta z & \text{for } j = -1, \dots, j_\mathrm{f} - 1, \\ q_\mathrm{u}(t) - \sum_{i=j+1}^{N} \mathcal{R}_i \Delta z & \text{for } j = j_\mathrm{f}, \dots, N-1, \\ q_\mathrm{u}(t) & \text{for } j = N, N+1. \end{cases} \tag{30}$$

The first bulk flow term qX of (28) can be handled by a standard upwind flux:

$$\mathcal{B}_{j+1/2} := \begin{cases} q_{j+1/2} X_{j+1} & \text{if } q_{j+1/2} \le 0, \\ q_{j+1/2} X_j & \text{if } q_{j+1/2} > 0, \end{cases} \qquad j = -1, \dots, N+1. \tag{31}$$

The rest of the terms of (28) are only non-zero (strictly) inside the SST. We define $\gamma_{j+1/2} := \gamma(z_{j+1/2})$ (recall that $\gamma(-H) = \gamma(B) = 0$) and define the numerical convective flux $G_{j+1/2}$ for $j = -1, \dots, N+1$ by means of the Godunov flux $\mathcal{G}$:

$$G_{j+1/2} := \gamma_{j+1/2} \mathcal{G}(X_j, X_{j+1}), \quad \text{where} \quad \mathcal{G}(u,v) := \begin{cases} \min\limits_{u \le X \le v} f_\mathrm{b}(X) & \text{if } u \le v, \\ \max\limits_{u \ge X \ge v} f_\mathrm{b}(X) & \text{if } u > v. \end{cases} \tag{32}$$

Analogously, the numerical compressive flux is

$$J_{j+1/2} := \gamma_{j+1/2} \big(D(X_{j+1}) - D(X_j) \big) / \Delta z, \quad j = -1, \dots, N+1.$$

Then the total flux (28) between cells j and $j+1$ is approximated by

$$F_{X,j+1/2} := \mathcal{B}_{j+1/2} + G_{j+1/2} - J_{j+1/2}, \qquad j = -1, \dots, N+1.$$

The corresponding flux of (26b) is $\boldsymbol{P}_{X,j+1/2} F_{X,j+1/2}$, where $\boldsymbol{P}_{X,j+1/2}$ needs to be defined. If $F_{X,j+1/2} > 0$, then particles move in the direction of the z-axis over the

boundary $z_{j+1/2}$, i.e. downwards. Then the values of $\boldsymbol{P}_{X,j+1/2}$ at the cell boundary are those coming from the left cell, i.e. $\boldsymbol{P}_{X,j}$. If $F_{X,j+1/2} \le 0$, then the particles move upwards and the values are $\boldsymbol{P}_{X,j+1}$. Conequently, following [14] we define

$$\boldsymbol{P}_{X,j+1/2} := \begin{cases} \boldsymbol{P}_{X,j+1} & \text{if } F_{X,j+1/2} \le 0, \\ \boldsymbol{P}_{X,j} & \text{if } F_{X,j+1/2} > 0, \end{cases} \qquad j = -1, \dots, N+1. \tag{33}$$

For the liquid percentage vector appearing in (26d), we use the same principle. We define $F_{L,j+1/2} := \rho_L q_{j+1/2} - r F_{X,j+1/2}$ for $j = -1, \dots, N+1$ and

$$\boldsymbol{P}_{L,j+1/2} := \begin{cases} \boldsymbol{P}_{L,j+1} & \text{if } F_{L,j+1/2} \le 0, \\ \boldsymbol{P}_{L,j} & \text{if } F_{L,j+1/2} > 0, \end{cases} \qquad j = -1, \dots, N+1.$$

We introduce the notation $[\Delta F]_j := F_{j+1/2} - F_{j-1/2}$ and let δ_{j,j_f} denote the Kronecker delta, which is 1 if $j = j_\mathrm{f}$ and zero otherwise. The conservation of mass for each layer gives the following method-of-lines equations (for $j = 0, \dots, N+1$):

$$\frac{\mathrm{d}X_j}{\mathrm{d}t} = -\frac{[\Delta F_X]_j}{\Delta z} + \delta_{j,j_\mathrm{f}} \frac{X_\mathrm{f} q_\mathrm{f}}{\Delta z} + \gamma_j \tilde{R}_{X,j}, \tag{34a}$$

$$\frac{\mathrm{d}(\boldsymbol{P}_{X,j} X_j)}{\mathrm{d}t} = -\frac{[\Delta(\boldsymbol{P}_X F_X)]_j}{\Delta z} + \delta_{j,j_\mathrm{f}} \frac{\boldsymbol{p}_{X,\mathrm{f}} X_\mathrm{f} q_\mathrm{f}}{\Delta z} + \gamma_j \boldsymbol{R}_{X,j}, \tag{34b}$$

$$L_j = \rho_L - r X_j,$$

$$\frac{\mathrm{d}(\boldsymbol{P}_{L,j} L_j)}{\mathrm{d}t} = -\frac{[\Delta(\boldsymbol{P}_L F_L)]_j}{\Delta z} + \delta_{j,j_\mathrm{f}} \frac{\boldsymbol{p}_{L,\mathrm{f}} L_\mathrm{f} q_\mathrm{f}}{\Delta z} + \gamma_j \boldsymbol{R}_{L,j}, \tag{34c}$$

$$P_L^{(k_L)} = 1 - \big(P_L^{(1)} + \cdots + P_L^{(k_L-1)}\big). \tag{34d}$$

If $X_j = 0$, i.e. there are no solids in layer j, then the value of $\boldsymbol{P}_{X,j}$ is irrelevant. Furthermore, note that in (34a) we have $\tilde{R}_{X,j} = \tilde{R}_X(\boldsymbol{C}_j, \boldsymbol{S}_j)$, where $\boldsymbol{C}_j = \boldsymbol{P}_{X,j} X_j$ and $\boldsymbol{S}_j = \bar{\boldsymbol{P}}_{L,j} L_j = \bar{\boldsymbol{P}}_{L,j}(\rho_L - r X_j)$, where $\bar{\boldsymbol{P}}_{L,j}$ is a vector containing the first $k_L - 1$ components of $\boldsymbol{P}_{L,j}$. The same holds for each component of $\boldsymbol{R}_{X,j}$ and $\boldsymbol{R}_{L,j}$. In (34c) and similar formulas below for the computation of $\boldsymbol{P}_L$ we skip the notation with a bar over all vectors. It is understood that the last equation of (34c) is replaced by (34d).

3.2. Explicit fully discrete scheme. First, we recall that the initial data for any (one-step) time discretization method can be obtained as is shown in Section 2.8.

If the final simulation time point is T, we let t_n, $n = 0, 1, \dots, n_T$, denote the discrete time points and $\Delta t = T/n_T$ the time step that should satisfy a certain CFL condition depending on the chosen time-integration method. Set $\lambda := \Delta t/\Delta z$. For explicit schemes, the right-hand sides of the equations are evaluated at time t_n. The value of a variable at time t_n is denoted by an upper index, e.g., X_j^n. For explicit Euler time integration of (34a)–(34c), we note in particular the approximation

$$\mathrm{d}(\boldsymbol{P}_{X,j} X_j)/\mathrm{d}t \approx \big(\boldsymbol{P}_{X,j}^{n+1} X_j^{n+1} - \boldsymbol{P}_{X,j}^n X_j^n\big)/\Delta t,$$

which implies the following explicit scheme:

$$X_j^{n+1} = X_j^n + \lambda\big(-[\Delta F_X^n]_j + \delta_{j,j_\mathrm{f}} X_\mathrm{f}^n q_\mathrm{f}^n\big) + \Delta t\, \gamma_j \tilde{R}_{X,j}^n, \tag{35a}$$

$$\boldsymbol{P}_{X,j}^{n+1} = \begin{cases} \text{irrelevant, e.g. } \boldsymbol{P}_{X,j}^n & \text{if } X_j^{n+1} = 0, \\ \big(1/X_j^{n+1}\big)\big[\boldsymbol{P}_{X,j}^n X_j^n + \lambda\big(-[\Delta(\boldsymbol{P}_X^n F_X^n)]_j \\ \quad + \delta_{j,j_\mathrm{f}} \boldsymbol{p}_{X,\mathrm{f}}^n X_\mathrm{f}^n q_\mathrm{f}^n A\big) + \Delta t\, \gamma_j \boldsymbol{R}_{X,j}^n\big] & \text{if } X_j^{n+1} > 0, \end{cases} \tag{35b}$$

$$L_j^{n+1} = \rho_L - rX_j^{n+1} \quad \text{(recall that always } L_j^{n+1} > 0\text{)}, \tag{35c}$$

$$\boldsymbol{P}_{L,j}^{n+1} = \frac{1}{L_j^{n+1}}\Big[\boldsymbol{P}_{L,j}^n L_j^n + \lambda\Big(- [\Delta(\boldsymbol{P}_L^n F_L^n)]_j + \delta_{j,j_\mathrm{f}} \boldsymbol{p}_{L,\mathrm{f}}^n L_\mathrm{f}^n q_\mathrm{f}^n A\Big) + \Delta t\, \gamma_j \boldsymbol{R}_{L,j}^n\Big], \tag{35d}$$

$$P_{L,j}^{(k_L),n+1} = 1 - \big(P_{L,j}^{(1),n+1} + \cdots + P_{L,j}^{(k_L-1),n+1}\big). \tag{35e}$$

The biological reactions do not only influence the variables locally via the reaction terms, but also globally via the additional bulk velocity term $q_{j+1/2}^{\mathrm{reac},n}$. In fact, a local volume increase or decrease at $z = z_0$ has an immediate influence for all $z < z_0$. In other words, the bulk velocity change $q^{\mathrm{reac}}(z; \boldsymbol{C}, \boldsymbol{S})$ given by (17) depends on the reactions in the interval $[z, B]$. For the numerical scheme, this means that the update formulas for the concentrations in a layer j_0 depends on the other concentrations in all layers $j > j_0$; see (30). We will see in Section 4 that this unfortunately means that the scheme is not monotone. The terms $\mathcal{R}_j$, $j = 1, \ldots, N$ in (29) destroy the monotonicity. Since these are negligibly small in wastewater treatment (see Section 5), we analyze the scheme when $q_{j+1/2}^{\mathrm{reac},n} := 0$ instead of (29).

3.3. CFL condition. We define the vector of unknowns $\boldsymbol{\mathcal{U}} := (\boldsymbol{p}_X, X, \boldsymbol{p}_L, L)$ and the following set (vectors in equalities should be interpreted component-wise):

$$\begin{aligned}\Omega := \big\{\boldsymbol{\mathcal{U}} \in \mathbb{R}^{k_X+k_L+2} : 0 \le \boldsymbol{p}_X, \boldsymbol{p}_L \le 1,\ 0 \le X \le X_\mathrm{m},\\ \rho_L - rX_\mathrm{m} \le L \le \rho_L,\ p_X^{(1)} + \cdots + p_X^{(k_X)} = 1,\ p_L^{(1)} + \cdots + p_L^{(k_L)} = 1\big\}.\end{aligned} \tag{36}$$

We define the following bounds (which are assumed to be finite):

$$\|f_\mathrm{b}\|_\infty := \max_{0\le X\le X_\mathrm{m}} |f_\mathrm{b}(X)|, \quad \|q\|_\infty := \max_{0\le t\le T} q_\mathrm{f}(t), \quad M_C := \sup_{\boldsymbol{\mathcal{U}}\in\Omega, 1\le i\le k_X} \big|\partial \tilde{R}_X/\partial C^{(i)}\big|,$$

$$M_S := \sup_{\boldsymbol{\mathcal{U}}\in\Omega, 1\le i\le k_L-1} \big|\partial \tilde{R}_X/\partial S^{(i)}\big|, \quad M_C^X := \sup_{\boldsymbol{\mathcal{U}}\in\Omega, 1\le i,k\le k_X} \big|\partial R_X^{(k)}/\partial C^{(i)}\big|,$$

$$M_S^X := \sup_{\boldsymbol{\mathcal{U}}\in\Omega, 1\le i,k\le k_L-1} \big|\partial R_X^{(k)}/S^{(i)}\big|, \quad M_S^L := \sup_{\boldsymbol{\mathcal{U}}\in\Omega, 1\le i,k\le k_L-1} \big|\partial R_L^{(k)}/S^{(i)}\big|$$

along with $M := M_C + rM_S$. The CFL condition for the scheme (35) is

$$\Delta t\big(\|q\|_\infty(\Delta z)^{-1} + \max(\beta_X, \beta_{\boldsymbol{P}_X}, \beta_{\boldsymbol{P}_L})\big) \le 1, \quad \text{where} \tag{CFL}$$

$$\beta_X := \frac{\|f_\mathrm{b}'\|_\infty}{\Delta z} + \frac{2\|d\|_\infty}{\Delta z^2} + M, \qquad \beta_{\boldsymbol{P}_X} := \frac{\|f_\mathrm{b}'\|_\infty}{\Delta z} + \frac{2\|d\|_\infty}{\Delta z^2} + M_C + M_C^X, \tag{37}$$

$$\beta_{\boldsymbol{P}_L} := \frac{\|f_\mathrm{b}\|_\infty}{\Delta z(\rho_X - X_\mathrm{m})} + \frac{2D(X_\mathrm{m})}{\Delta z^2(\rho_X - X_\mathrm{m})} + M_S^L + rM_S. \tag{38}$$

4. Properties of the numerical scheme. With $\eta := \lambda/\Delta z = \Delta t/\Delta z^2$ the update formula (35a) reads for each layer:

$$\begin{aligned}
X_0^{n+1} &= X_0^n - \lambda[\Delta\mathcal{B}^n]_0,\\
X_1^{n+1} &= X_1^n - \lambda\big([\Delta\mathcal{B}^n]_1 + \mathcal{G}(X_1^n, X_2^n)\big) + \eta\big(D(X_2^n) - D(X_1^n)\big) + \Delta t\, \tilde{R}_{X,1}^n,\\
X_j^{n+1} &= X_j^n - \lambda\big([\Delta\mathcal{B}^n]_j + \mathcal{G}(X_j^n, X_{j+1}^n) - \mathcal{G}(X_{j-1}^n, X_j^n)\big)\\
&\quad + \eta\big(D(X_{j+1}^n) - 2D(X_j^n) + D(X_{j-1}^n)\big) + \lambda\delta_{j,j_\mathrm{f}} X_\mathrm{f}^n q_\mathrm{f}^n + \Delta t\, \tilde{R}_{X,j}^n, \quad j = 2, \ldots, N-1,\\
X_N^{n+1} &= X_N^n - \lambda\big([\Delta\mathcal{B}^n]_N - \mathcal{G}(X_{N-1}^n, X_N^n)\big) - \eta\big(D(X_N^n) - D(X_{N-1}^n)\big) + \Delta t\, \tilde{R}_{X,N}^n\\
X_{N+1}^{n+1} &= X_{N+1}^n - \lambda[\Delta\mathcal{B}^n]_{N+1}.
\end{aligned}$$

To be able to prove an invariant region property for each variable, we want every formula to be a monotone function of each argument, i.e., we wish to have $\partial_{X_k^n} X_j^{n+1} \geq 0$ for all j, k. For $j = k$, this can be achieved by invoking (CFL). The problematic terms above are $\lambda[\Delta \mathcal{B}^n]_j$ since they contain the bulk velocity reaction function q^{reac} in (17). To see this, we let the characteristic function χ_I be equal to 1 if the statement I is true, otherwise 0. Then $\mathcal{B}_{j+1/2} = X_{j+1} q_{j+1/2} \chi_{q_{j+1/2} \leq 0} + X_j q_{j+1/2} \chi_{q_{j+1/2} > 0}$ and hence, for $j = 0, \dots, N-1$ and $k = j+2, \dots, N+1$, we have

$$\begin{aligned}\partial_{X_k} X_j^{n+1} = -\lambda \partial_{X_k} [\Delta \mathcal{B}]_j = -\lambda \big(&(X_{j+1} \chi_{q_{j+1/2} \leq 0} + X_j \chi_{q_{j+1/2} > 0}) \partial_{X_k} q_{j+1/2} \\ &+ (X_j \chi_{q_{j-1/2} \leq 0} + X_{j-1} \chi_{q_{j-1/2} > 0}) \partial_{X_k} q_{j-1/2} \big).\end{aligned}$$

The derivatives of $q_{j+1/2}^n$ can have any sign due to the reaction terms. We therefore confine the analysis to the scheme when we set $\mathcal{R}_j := 0$, $j = 1, \dots, N$ in (29), i.e. $q_{j+1/2}^{\mathrm{reac}} := 0$. Then $q_{j+1/2}$ depends only on time and (35) becomes a three-point scheme. We write the update formulas (35a), (35b) and (35d) for $j = 0, \dots, N+1$ as

$$\begin{aligned} X_j^{n+1} &= \mathcal{H}_X \big(X_{j-1}^n, X_j^n, X_{j+1}^n \big), \\ P_{X,j}^{(i),n+1} &= \mathcal{P}_i \big(P_{X,j-1}^{(i),n}, P_{X,j}^{(i),n}, P_{X,j+1}^{(i),n} \big), \quad i = 1, \dots, k_X, \\ P_{L,j}^{(i),n+1} &= \mathcal{Q}_i \big(P_{L,j-1}^{(i),n}, P_{L,j}^{(i),n}, P_{L,j+1}^{(i),n} \big), \quad i = 1, \dots, k_L. \end{aligned}$$

The variables $\boldsymbol{P}_{X,j}^n$ and $\boldsymbol{P}_{L,j}^n$ are considered as constants within $\mathcal{H}_X$ since they were updated at the previous time point. However, because of the algebraic equation (35c), the source term in the expression for $\mathcal{H}_X$ should be interpreted as

$$\boldsymbol{R}_{X,j}^n = \boldsymbol{R}_X^n (\boldsymbol{P}_{X,j}^n X_j^n, \bar{\boldsymbol{P}}_{L,j}^n (\rho_L - r X_j^n)).$$

Moreover, $\mathcal{P}_i$ contains X_j^{n+1}, which depends on $\boldsymbol{P}_X^{(i)}$ via the reaction term. A similar property holds for $\mathcal{Q}_i$.

LEMMA 5. *Assume that $0 \leq X_j \leq X_{\mathrm{m}}$ for all j. Then the Godunov flux $\mathcal{G}_{j+1/2} = \mathcal{G}(X_j, X_{j+1})$, see (32), applied on $0 \leq f_{\mathrm{b}} \in C^1$ satisfies*

$$\begin{aligned} &- \|f_{\mathrm{b}}'\|_\infty \leq \partial_{X_{j+1}} \mathcal{G}_{j+1/2} \leq 0 \leq \partial_{X_j} \mathcal{G}_{j+1/2} \leq \|f_{\mathrm{b}}'\|_\infty, \\ &\big|\partial_{X_j} [\Delta \mathcal{G}]_j\big| \leq \|f_{\mathrm{b}}'\|_\infty, \quad \frac{\mathcal{G}_{j+1/2}}{X_j} \leq \|f_{\mathrm{b}}'\|_\infty, \quad \frac{\mathcal{G}_{j+1/2}}{X_{j+1}} \leq \|f_{\mathrm{b}}'\|_\infty. \end{aligned}$$

Proof. If $X_j \leq X_{j+1}$, then $\mathcal{G}_{j+1/2} = \min\{f_{\mathrm{b}}(X_j), f_{\mathrm{b}}(\xi), f_{\mathrm{b}}(X_{j+1})\}$, where $\xi \in (X_j, X_{j+1})$ is a (possible) stationary point of f_{b}. If $\mathcal{G}_{j+1/2} = f_{\mathrm{b}}(X_j)$, then X_j is the minimum point and the left endpoint of the interval, hence $\partial_{X_j} \mathcal{G}_{j+1/2} = f_{\mathrm{b}}'(X_j) \geq 0$. Otherwise, $\partial_{X_j} \mathcal{G}_{j+1/2} = 0$ holds. Similarly, if $X_j > X_{j+1}$, then $\partial_{X_j} \mathcal{G}_{j+1/2} = 0$ or $= f_{\mathrm{b}}'(X_j) \geq 0$ (the right endpoint X_j is a maximum point). Analogously, $\partial_{X_{j+1}} \mathcal{G}_{j+1/2} = 0$ or $= f_{\mathrm{b}}'(X_{j+1}) \leq 0$. Combining these results, we get (for $X_j^n \neq X_{j+1}^n$)

$$\partial_{X_j} [\Delta \mathcal{G}]_j \in \{f_{\mathrm{b}}'(X_j), 0, -f_{\mathrm{b}}'(X_j)\}.$$

Assume again $X_j \leq X_{j+1}$, so that $\mathcal{G}_{j+1/2} = \min\{f_{\mathrm{b}}(X_j), f_{\mathrm{b}}(\xi), f_{\mathrm{b}}(X_{j+1})\}$. Then both $\mathcal{G}_{j+1/2}/X_j \leq f_{\mathrm{b}}(X_j)/X_j$ and $\mathcal{G}_{j+1/2}/X_{j+1} \leq f_{\mathrm{b}}(X_{j+1})/X_{j+1}$ hold. If $X_j > X_{j+1}$, then $\mathcal{G}_{j+1/2} = \max\{f_{\mathrm{b}}(X_j^n), f_{\mathrm{b}}(\xi), f_{\mathrm{b}}(X_{j+1}^n)\}$ where $\xi \in (X_{j+1}, X_j)$ is a possible stationary point. Then we have

$$\frac{\mathcal{G}_{j+1/2}}{X_{j+1}} \leq \frac{\mathcal{G}_{j+1/2}}{X_j} = \begin{cases} \text{either} & f_{\mathrm{b}}(X_j)/X_j, \\ \text{or} & f_{\mathrm{b}}(\xi)/X_j \leq f_{\mathrm{b}}(\xi)/\xi, \\ \text{or} & f_{\mathrm{b}}(X_{j+1})/X_j \leq f_{\mathrm{b}}(X_{j+1})/X_{j+1}. \end{cases}$$

For any $X \in (0, X_\mathrm{m})$, take $\bar\xi \in (0, X)$ according to the mean-value theorem so that

$$f_\mathrm{b}(X)/X = \big(f_\mathrm{b}(X) - f_\mathrm{b}(0)\big)/X = f_\mathrm{b}'(\bar\xi) \le \|f_\mathrm{b}'\|_\infty. \qquad \square$$

We define the vector of unknown discrete variables $\boldsymbol{\mathcal{U}}_j^n := (\boldsymbol{P}_{X,j}^n, X_j^n, \boldsymbol{P}_{L,j}^n, L_j^n)$.

LEMMA 6. *Assume that $\boldsymbol{\mathcal{U}}_j^n \in \Omega$ for all j. Then the following holds:*

$$\left|\frac{\partial \tilde R_{X,j}}{\partial X_k}\right| \begin{cases} \le M & \text{if } k = j, \\ = 0 & \text{if } k \ne j, \end{cases} \qquad \left|\frac{\partial \tilde R_{X,j}}{\partial P_{X,k}^{(i)}}\right| = X_k \left|\frac{\partial \tilde R_{X,j}}{\partial C_k^{(i)}}\right| \begin{cases} \le X_j M_C & \text{if } k = j, \\ = 0 & \text{if } k \ne j. \end{cases}$$

Proof. The cases $k \ne j$ are trivial. Assume that $k = j$ and differentiate

$$\partial_{X_j} \tilde R_{X,j} = \partial_{X_j} \tilde R_X\big(\boldsymbol{P}_{X,j} X_j, \bar{\boldsymbol{P}}_{L,j}(\rho_L - r X_j)\big) = \boldsymbol{P}_{X,j}^\mathrm{T} \nabla_{\boldsymbol{C}} \tilde R_X - r \bar{\boldsymbol{P}}_{L,j}^\mathrm{T} \nabla_{\boldsymbol{S}} \tilde R_X,$$

where the first term is estimated by

$$|\boldsymbol{P}_{X,j}^\mathrm{T} \nabla_{\boldsymbol{C}} \tilde R_X| \le \sum_{i=1}^{k_X} |P_{X,j}^{(i)}| \left|\partial_{C^{(i)}} \tilde R_X\right| \le M_C \sum_{i=1}^{k_X} |P_{X,j}^{(i)}| = M_C,$$

and the second term similarly. The derivative $|\partial_{P_{X,k}^{(i)}} \tilde R_{X,j}|$ is handled similarly. $\square$

LEMMA 7. *If $\boldsymbol{\mathcal{U}}_j^n \in \Omega$, $q_{j+1/2}^{\mathrm{reac},n} := 0$ for all j and (CFL) holds, then $\mathcal{H}_X$ is a non-decreasing function in each variable, i.e., the update formula (35a) is monotone.*

Proof. We define $a^+ := \max\{a, 0\}$ and $a^- := \min\{a, 0\}$. Then

$$\mathcal{B}_{j+1/2}^n = X_{j+1}^n q_{j+1/2}^n \chi_{q_{j+1/2}^n \le 0} + X_j^n q_{j+1/2}^n \chi_{q_{j+1/2}^n > 0} = X_{j+1}\big(q_{j+1/2}^n\big)^- + X_j\big(q_{j+1/2}^n\big)^+.$$

Furthermore, with $q_{j+1/2}^{n,+} := (q_{j+1/2}^n)^+$ etc., we have

$$\begin{aligned} \partial_{X_j^n}[\Delta \mathcal{B}^n]_j &= \partial_{X_j^n}\big(X_{j+1}^n q_{j+1/2}^{n,-} + X_j^n q_{j+1/2}^{n,+} - X_j^n q_{j-1/2}^{n,-} - X_{j-1}^n q_{j-1/2}^{n,+}\big) \\ &= q_{j+1/2}^{n,+} - q_{j-1/2}^{n,-} \le q_{j_\mathrm{f}+1/2}^{n,+} - q_{j_\mathrm{f}-1/2}^{n,-} = q_\mathrm{u}^n + q_\mathrm{e}^n = q_\mathrm{f}^n \le \|q\|_\infty. \end{aligned}$$

Differentiation of (35a) and utilization of (CFL) and Lemmas 5 and 6 imply

$$\begin{aligned} \partial_{X_0^n} X_0^{n+1} &= 1 - \lambda \partial_{X_0^n}[\Delta \mathcal{B}^n]_0 \ge 1 - \lambda \|q\|_\infty \ge 0, \\ \partial_{X_1^n} X_0^{n+1} &= -\lambda q_{1/2}^{n,-} \ge 0, \qquad \partial_{X_0^n} X_1^{n+1} = \lambda q_{1/2}^{n,+} \ge 0, \\ \partial_{X_1^n} X_1^{n+1} &= 1 - \lambda\big(\partial_{X_1^n}[\Delta \mathcal{B}^n]_1 + \partial_{X_1^n} \mathcal{G}(X_1^n, X_2^n)\big) - \eta d(X_1^n) + \Delta t\, \partial_{X_1^n} \tilde R_{X,1}^n \\ &\ge 1 - \big(\lambda\big(\|q\|_\infty + \|f_\mathrm{b}'\|_\infty\big) + \eta \|d\|_\infty + \Delta t\, M\big) \ge 0, \\ \partial_{X_2^n} X_1^{n+1} &= \lambda\big(-q_{3/2}^{n,-} - \partial_{X_2^n} \mathcal{G}(X_1^n, X_2^n)\big) + \eta d(X_2^n) \ge 0, \\ \partial_{X_{j-1}^n} X_j^{n+1} &= \lambda\big(q_{j-1/2}^{n,+} + \partial_{X_{j-1}^n} \mathcal{G}(X_{j-1}^n, X_j^n)\big) + \eta d(X_{j-1}^n) \ge 0, \quad j = 2, \dots, N-1, \\ \partial_{X_j^n} X_j^{n+1} &= 1 - \lambda\big(\partial_{X_j^n}[\Delta \mathcal{B}^n]_j + \partial_{X_j^n}[\Delta \mathcal{G}^n]_j\big) - 2\eta d(X_j^n) + \Delta t\, \partial_{X_j^n} \tilde R_{X,j}^n \\ &\ge 1 - \big(\lambda(\|q\|_\infty + \|f_\mathrm{b}'\|_\infty) + 2\eta \|d\|_\infty + \Delta t\, M\big) \ge 0, \quad j = 2, \dots, N-1, \\ \partial_{X_{j+1}^n} X_j^{n+1} &= -\lambda\big(q_{j+1/2}^{n,-} + \partial_{X_{j+1}^n} \mathcal{G}(X_j^n, X_{j+1}^n)\big) + \eta d(X_{j+1}^n) \ge 0, \quad j = 2, \dots, N-1. \end{aligned}$$

The remaining derivatives at the boundary $z = B$ are symmetric to those at $z = -H$. $\square$

LEMMA 8. *If $\boldsymbol{\mathcal{U}}_j^n \in \Omega$, $q_{j+1/2}^{\mathrm{reac},n} := 0$ for all j, and (CFL) holds, then $\mathcal{P}_i$ is a non-decreasing function in each variable, i.e., the update formula for $\boldsymbol{P}_{X,j}^n$ (35b) (in which X_j^{n+1} is a function of $\boldsymbol{P}_{X,j}^n$ by (35a)) is monotone.*

Proof. If $X_j^{n+1} = 0$, then the value of $\boldsymbol{P}_{X,j}^{n+1}$ is irrelevant, since only the product $X_j^{n+1}\boldsymbol{P}_{X,j}^{n+1} = 0$ appears in the next iteration so we assume that $X_j^{n+1} > 0$. Before differentiating (35b), we write out:

$$\begin{aligned}[\Delta(\boldsymbol{P}_X^n F_X^n)]_j =& \boldsymbol{P}_{X,j+1/2}^n F_{X,j+1/2}^n - \boldsymbol{P}_{X,j-1/2}^n F_{X,j-1/2}^n \\ =& \boldsymbol{P}_{X,j+1}^n F_{X,j+1/2}^{n,-} + \boldsymbol{P}_{X,j}^n F_{X,j+1/2}^{n,+} - \boldsymbol{P}_{X,j}^n F_{X,j-1/2}^{n,-} - \boldsymbol{P}_{X,j-1}^n F_{X,j-1/2}^{n,+}.\end{aligned}$$

We write (35b) as $\boldsymbol{P}_{X,j}^{n+1} = \boldsymbol{\Psi}_X(\boldsymbol{P}_{X,j-1}^n, \boldsymbol{P}_{X,j}^n, \boldsymbol{P}_{X,j+1}^n)/X_j^{n+1}(\boldsymbol{P}_{X,j}^n)$. The nonzero derivatives are the following for $k = 0, \dots, N+1$:

$$\begin{aligned}&\frac{\partial P_{X,j}^{(k),n+1}}{\partial P_{X,j-1}^{(i),n}} = \frac{\lambda}{X_j^{n+1}} F_{X,j-1/2}^{n,+} \geq 0, \qquad \frac{\partial P_{X,j}^{(k),n+1}}{\partial P_{X,j-1}^{(i),n}} = \frac{\lambda}{X_j^{n+1}}\big(-F_{X,j-1/2}^{n,-}\big) \geq 0, \\ &\frac{\partial P_{X,j}^{(k),n+1}}{\partial P_{X,j}^{(i),n}} = -\frac{\Psi_X^{(k),n}}{(X_j^{n+1})^2}\frac{\partial X_j^{n+1}}{\partial P_{X,j}^{(i),n}} + \frac{1}{X_j^{n+1}}\frac{\partial \Psi_X^{(k),n}}{\partial P_{X,j}^{(i),n}}.\end{aligned} \tag{39}$$

The first term of (39) is estimated with Lemma 6 and the fact that $\Psi_X^{(k),n} \leq X_j^{n+1}$:

$$-\frac{\Psi_X^{(k),n}}{(X_j^{n+1})^2}\frac{\partial X_j^{n+1}}{\partial P_{X,j}^{(i),n}} = -\frac{\Psi_X^{(k),n}}{(X_j^{n+1})^2}\Delta t\, X_j^n \frac{\partial \tilde{R}_{X,j}^n}{\partial C_j^{(i),n}} \geq -\frac{X_j^n}{X_j^{n+1}}\Delta t\, M_C.$$

The second term of (39) is

$$\frac{1}{X_j^{n+1}}\frac{\partial \Psi_X^{(k),n}}{\partial P_{X,j}^{(i),n}} = \frac{1}{X_j^{n+1}}\left(X_j^n - \lambda\big\{F_{X,j+1/2}^{n,+} - F_{X,j-1/2}^{n,-}\big\} + \Delta t\,\gamma_j \frac{\partial R_{X,j}^{(k),n}}{\partial P_{X,j}^{(i),n}}\right).$$

The last term is estimated as

$$\frac{1}{X_j^{n+1}}\Delta t\,\gamma_j \frac{\partial R_{X,j}^{(k),n}}{\partial P_{X,j}^{(i),n}} = \frac{X_j^n}{X_j^{n+1}}\Delta t\,\gamma_j \frac{\partial R_{X,j}^{(k),n}}{\partial C_j^{(i),n}} \geq -\frac{X_j^n}{X_j^{n+1}}\Delta t\, M_C^X.$$

To estimate the expression within curled brackets, we note that $-a^- = (-a)^+$, $(a+b)^+ \leq a^+ + b^+$ and start with the first of three terms corresponding to $F_X = \mathcal{B} + G - J$:

$$\begin{aligned}\mathcal{B}_{j+1/2}^{n,+} + (-\mathcal{B}_{j-1/2}^n)^+ &= \big(X_{j+1}^n q_{j+1/2}^{n,-} + X_j^n q_{j+1/2}^{n,+}\big)^+ + \big(-X_j^n q_{j-1/2}^{n,-} - X_{j-1}^n q_{j-1/2}^{n,+}\big)^+ \\ &\leq X_j^n(q_{j+1/2}^{n,+} - q_{j-1/2}^{n,-}) \leq X_j^n(q_{j_{\mathrm{f}}+1/2}^{n,+} - q_{j_{\mathrm{f}}+1/2}^{n,-}) \\ &= X_j^n(q_{\mathrm{u}}^n + q_{\mathrm{e}}^n) = X_j^n q_{\mathrm{f}}^n \leq X_j^n \|q\|_\infty.\end{aligned}$$

Since $\mathcal{G}(u,v) > 0$ whenever $f_{\mathrm{b}} > 0$ and using Lemma 5, we obtain

$$G_{j+1/2}^{n,+} + (-G_{j-1/2}^n)^+ = G_{j+1/2}^{n,+} = G_{j+1/2}^n \leq X_j^n \|f_{\mathrm{b}}'\|_\infty.$$

The term corresponding to $-J$ is estimated by utilizing that $D(X)$ is a non-decreasing function, which is zero for $X \leq X_{\mathrm{c}}$:

$$\begin{aligned}(-J_{j+1/2}^{n,+})^+ + J_{j-1/2}^{n,+} &= \frac{1}{\Delta z}\Big(\big(D(X_j^n) - D(X_{j+1}^n)\big)^+ + \big(D(X_j^n) - D(X_{j-1}^n)\big)^+\Big) \\ &\leq \frac{1}{\Delta z} 2D(X_j^n) = \frac{2}{\Delta z}\int_{X_{\mathrm{c}}}^{X_j^n} d(s)\,\mathrm{d}s \leq X_j^n \frac{2\|d\|_\infty}{\Delta z}.\end{aligned} \tag{40}$$

The CFL condition (CFL) now implies that

$$\frac{\partial P_{X,j}^{(k),n+1}}{\partial P_{X,j}^{(i),n}} \geq \frac{X_j^n}{X_j^{n+1}} \left[1 - \left(\lambda\big(\|q\|_\infty + \|f_\mathrm{b}'\|_\infty\big) + 2\eta\|d\|_\infty + \Delta t\,(M_C + M_C^X)\right)\right] \geq 0. \qquad \square$$

LEMMA 9. *If $\boldsymbol{\mathcal{U}}_j^n \in \Omega$, $q_{j+1/2}^{\mathrm{reac},n} := 0$ for all j and (CFL) holds, then $\mathcal{Q}_i$ is a non-decreasing function in each variable, i.e., the update formula for $\boldsymbol{P}_{L,j}^n$ (35d) (in which L_j^{n+1} is a function of $\boldsymbol{P}_{L,j}^n$ via (35c) and (35a)) is monotone.*

Proof. We follow the proof of Lemma 8 and skip some details. We write (35d) as

$$\boldsymbol{P}_{L,j}^{n+1} = \frac{\boldsymbol{\Psi}_L(\boldsymbol{P}_{L,j-1}^n, \boldsymbol{P}_{L,j}^n, \boldsymbol{P}_{L,j+1}^n)}{L_j^{n+1}(\boldsymbol{P}_{L,j}^n)} = \frac{\boldsymbol{\Psi}_L(\boldsymbol{P}_{L,j-1}^n, \boldsymbol{P}_{L,j}^n, \boldsymbol{P}_{L,j-1}^n)}{\rho_L - rX_j^{n+1}(\boldsymbol{P}_{L,j}^n)}$$

and differentiate with respect to layer j:

$$\frac{\partial P_{L,j}^{(k),n+1}}{\partial P_{L,j}^{(i),n}} = -\frac{\Psi_L^{(k),n}(\boldsymbol{P}_{L,j}^n)}{(L_j^{n+1})^2}\frac{\partial L_j^{n+1}}{\partial P_{L,j}^{(i),n}} + \frac{1}{L_j^{n+1}}\frac{\partial \Psi_L^{(k),n}}{\partial P_{L,j}^{(i),n}}. \tag{41}$$

The first term of (41) is estimated by means of Lemma 6:

$$-\frac{\Psi_L^{(k),n}}{(L_j^{n+1})^2}\frac{\partial L_j^{n+1}}{\partial P_{L,j}^{(i),n}} = \frac{\Psi_L^{(k),n} r}{(L_j^{n+1})^2}\frac{\partial X_j^{n+1}}{\partial P_{L,j}^{(i),n}} = \frac{\Psi_L^{(k),n} r\Delta t\, L_j^n}{(L_j^{n+1})^2}\frac{\partial \tilde{R}_{X,j}^{(k),n}}{\partial S_j^{(i),n}} \geq -\frac{r\Delta t\, L_j^n}{L_j^{n+1}} M_S.$$

For the second term of (41), we note that

$$\begin{aligned} F_{L,j+1/2}^{n,+} &= (q_{j+1/2}^n \rho_L - rF_{X,j+1/2}^n)^+ \\ &= (q_{j+1/2}^n \rho_L - r\mathcal{B}_{j+1/2}^n - rG_{j+1/2}^n + rJ_{j+1/2}^n)^+ \leq \mathcal{T}_1 + rJ_{j+1/2}^{n,+}, \end{aligned}$$

where $\mathcal{T}_1 := (q_{j+1/2}^n \rho_L - r\mathcal{B}_{j+1/2}^n)^+$. Similarly, we obtain

$$(-F_{L,j-1/2}^{n,+})^+ \leq \mathcal{T}_2 + rG_{j-1/2}^{n,+} + r(-J_{j-1/2}^n)^+, \quad \mathcal{T}_2 := (-q_{j-1/2}^n \rho_L + r\mathcal{B}_{j-1/2}^n)^+.$$

Utilizing $q_{j+1/2}^n = q_{j+1/2}^{n,+} + q_{j+1/2}^{n,-}$ and $\mathcal{B}_{j+1/2}^n = X_{j+1} q_{j+1/2}^{n,-} + X_j q_{j+1/2}^{n,+}$, we have

$$\begin{aligned} \mathcal{T}_1 + \mathcal{T}_2 &= \big(q_{j+1/2}^{n,+}(\rho_L - rX_j^n) + q_{j+1/2}^{n,-}(\rho_L - rX_{j+1}^n)\big)^+ \\ &\quad + \big(-q_{j-1/2}^{n,+}(\rho_L - rX_{j-1}^n) - q_{j-1/2}^{n,-}(\rho_L - rX_j^n)\big)^+ \\ &= \big(q_{j+1/2}^{n,+} L_j^n + q_{j+1/2}^{n,-} L_j^{n+1}\big)^+ + \big(-q_{j-1/2}^{n,+} L_{j-1}^n - q_{j-1/2}^{n,-} L_j^n\big)^+ \\ &\leq (q_{j+1/2}^{n,+} - q_{j-1/2}^{n,-}) L_j^n \leq L_j^n \|q\|_\infty. \end{aligned}$$

For the rest of the terms, we have from Lemma 6 and (40):

$$\begin{aligned} rG_{j-1/2}^{n,+} \leq r\|f_\mathrm{b}\|_\infty = \frac{L_j^n}{\rho_L - rX_j^n} r\|f_\mathrm{b}\|_\infty \leq \frac{L_j^n}{\rho_X - X_\mathrm{m}}\|f_\mathrm{b}\|_\infty, \\ r(-J_{j+1/2}^{n,+})^+ + rJ_{j-1/2}^{n,+} \leq \frac{r2D(X_j^n)}{\Delta z} \leq \frac{L_j^n}{\rho_X - X_\mathrm{m}}\frac{2D(X_\mathrm{m})}{\Delta z}. \end{aligned}$$

TABLE 1
Coefficients for the calculation of the CFL condition (CFL).

N	Δz [m]	β_X [s^{-1}]	$\beta_{\boldsymbol{P}_X}$ [s^{-1}]	$\beta_{\boldsymbol{P}_L}$ [s^{-1}]	Δt [s]
10	4.000e-01	3.17614e+00	5.40438e-03	8.14990	0.121486
30	1.333e-01	3.19219e+00	2.14497e-02	8.14991	0.121486
90	4.444e-02	3.28380e+00	1.13058e-01	8.14993	0.121486
270	1.481e-02	3.94987e+00	7.79132e-01	8.15001	0.121484
405	9.877e-03	4.83456e+00	1.66382e+00	8.15007	0.121484
810	4.938e-03	9.46933e+00	6.29859e+00	8.15024	0.104558
2430	1.646e-03	5.77189e+01	5.45482e+01	8.15094	0.017154

The reaction term is handled as

$$\Delta t\,\gamma_j \frac{\partial R_{L,j}^{(k),n}}{\partial P_{L,j}^{(i),n}} = \Delta t\,\gamma_j L_j^n \frac{\partial R_{L,j}^{(k),n}}{\partial S_j^{(i),n}} \geq -\Delta t\, L_j^n M_S^L.$$

The CFL condition implies

$$\frac{\partial P_{L,j}^{(k),n+1}}{\partial P_{L,j}^{(i),n}} \geq \frac{L_j^n}{L_j^{n+1}}\left[1 - \lambda\|q\|_\infty - \frac{\lambda\|f_\mathrm{b}\|_\infty + 2\eta D(X_\mathrm{m})}{\rho_X - X_\mathrm{m}} - \Delta t(rM_S + M_S^L)\right] \geq 0. \quad \square$$

THEOREM 2. *If* (7) *and* (CFL) *hold, then* Ω *is invariant under the scheme* (35) *with* $q_{j+1/2}^{\mathrm{reac},n} := 0$ *for all* j, *i.e.,* $\boldsymbol{\mathcal{U}}_j^n \in \Omega \Rightarrow \boldsymbol{\mathcal{U}}_j^{n+1} \in \Omega$ *for all* j *and* n.

Proof. The monotonicity of $\mathcal{H}_X$ and the assumptions (7) imply that, for $j \neq j_\mathrm{f}$,

$$0 = \mathcal{H}_X(0,0,0) \leq X_j^{n+1} = \mathcal{H}_X(X_{j-1}^n, X_j^n, X_{j+1}^n) \leq \mathcal{H}_X(X_\mathrm{m}, X_\mathrm{m}, X_\mathrm{m}) = X_\mathrm{m}$$

and for $j = j_\mathrm{f}$ we have

$$\begin{aligned} 0 \leq \Delta t\, X_\mathrm{f} q_\mathrm{f} = \mathcal{H}_X(0,0,0) \leq X_j^{n+1} = \mathcal{H}_X(X_{j-1}^n, X_j^n, X_{j+1}^n) \leq \mathcal{H}_X(X_\mathrm{m}, X_\mathrm{m}, X_\mathrm{m}) \\ = X_\mathrm{m} - \lambda\big(q_\mathrm{u} X_\mathrm{m} - (q_\mathrm{u} - q_\mathrm{f})X_\mathrm{m}\big) + \lambda X_\mathrm{f} q_\mathrm{f} = X_\mathrm{m} - \lambda q_\mathrm{f}(X_\mathrm{m} - X_\mathrm{f}) \leq X_\mathrm{m}. \end{aligned}$$

Then we get $\rho_L - rX_\mathrm{m} \leq L_j^{n+1} = \rho_L - rX_j^{n+1} \leq \rho_L$. Similarly, the monotonicity properties of both $\mathcal{P}_i$ and $\mathcal{Q}_i$ imply the positivity preservation of $\boldsymbol{P}_{X,j}^n$ and $\boldsymbol{P}_{L,j}^n$. Furthermore, following the beginning of the proof of Lemma 8 we easily see that

$$\sum_{i=1}^{k_X} \Delta[P_X^{(i),n} F_X^n]_j = F_{X,j+1/2}^n - F_{X,j-1/2}^n = [\Delta F_X^n]_j.$$

Summing all equations in (35b) and using (35a), we get $\sum_{i=1}^{k_X} P_{X,j}^{(i),n+1} = 1$. In view of $\boldsymbol{P}_{X,j}^{n+1} \geq 0$ we obtain $\boldsymbol{P}_{X,j}^{n+1} \leq 1$. Since $\sum_{i=1}^{k_L} P_{L,j}^{(i),n+1} = 1$ by (35e), we get in the same way $0 \leq \boldsymbol{P}_{L,j}^{n+1} \leq 1$. $\square$

5. Numerical examples.

5.1. Preliminaries.

For the simulations, we choose the constitutive functions

$$v_\mathrm{hs}(X) = \frac{v_0}{1 + (X/\bar{X})^r} Z(X), \qquad \sigma_\mathrm{e}(X) = \begin{cases} 0 & \text{for } X < X_\mathrm{c}, \\ \alpha(X - X_\mathrm{c}) & \text{for } X > X_\mathrm{c}, \end{cases}$$

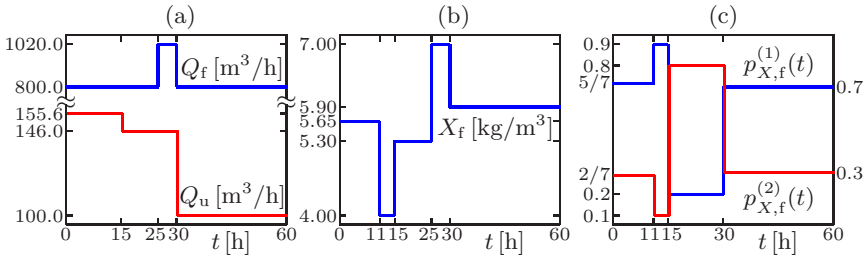

FIG. 2. *Examples 1 (a, b) and 2 (c): (a) volumetric flows, (b) solids feed concentration, (c) substrate feed percentages. The piecewise constant values and time points of changes are indicated.*

where $v_0 = 1.76 \times 10^{-3}\,\mathrm{m/s}$, $\bar{X} = 3.87\,\mathrm{kg/m^3}$, $\bar{r} = 3.58$, $\alpha = 0.2\,\mathrm{m^2/s^2}$ and $X_{\mathrm{c}} = 5\,\mathrm{kg/m^3}$. The continuous function $Z(X)$ should be equal to one for low concentrations and decrease to zero at some large concentration so that the second technical assumption in (7) is satisfied. The function $Z(X)$ should not influence the condition (CFL). We have used $Z(X) \equiv 1$ for all simulations and still obtained bounded solutions. Hence, after some trial simulations, the maximum concentration X_{m} can be defined and used in (CFL). We have used $X_{\mathrm{m}} = 30\,\mathrm{kg/m^3}$. Other constants used are $A = 400\,\mathrm{m^2}$, $\rho_X = 1050\,\mathrm{kg/m^3}$, $\rho_L = 998\,\mathrm{kg/m^3}$ and $g = 9.81\,\mathrm{m/s^2}$.

The biological reactions are those of a model of denitrification, which is conversion of bound nitrogen to free nitrogen ($\mathrm{N_2}$) that occurs in SSTs in wastewater treatment [4]. The $k_X = 2$ particulate concentrations are X_{OHO} (ordinary heterotrophic organisms) and X_{U} (undegradable organics), and the $k_L - 1 = 3$ soluble concentrations $S_{\mathrm{NO_3}}$ (nitrite), S_{S} (readily biodegradable substrate) and $S_{\mathrm{N_2}}$ (nitrogen), so that $\boldsymbol{p}_X X = \boldsymbol{C} = (X_{\mathrm{OHO}}, X_{\mathrm{U}})^{\mathrm{T}}$ and $\boldsymbol{S} = (S_{\mathrm{NO_3}}, S_{\mathrm{S}}, S_{\mathrm{N_2}})^{\mathrm{T}}$. The reaction terms are

$$\boldsymbol{R}_X = X_{\mathrm{OHO}} \begin{pmatrix} \mu(\boldsymbol{S}) - b \\ f_{\mathrm{P}} b \end{pmatrix} Z(X), \quad \boldsymbol{R}_L = X_{\mathrm{OHO}} \begin{pmatrix} -\frac{1-Y}{2.86Y}\mu(\boldsymbol{S}) \\ -\frac{1}{Y}\mu(\boldsymbol{S}) + (1 - f_{\mathrm{P}})b \\ \frac{1-Y}{2.86Y}\mu(\boldsymbol{S}) \\ 0 \end{pmatrix},$$

where $Y = 0.67$ is a yield factor, $b = 6.94 \times 10^{-6}\,\mathrm{s^{-1}}$ is the decay rate of heterotrophic organisms and $f_{\mathrm{P}} = 0.2$ is the portion of these that decays to undegradable organics. The specific growth rate function is

$$\mu(\boldsymbol{S}) := \mu_{\max} \frac{S_{\mathrm{NO_3}}}{K_{\mathrm{NO_3}} + S_{\mathrm{NO_3}}} \frac{S_{\mathrm{S}}}{K_{\mathrm{S}} + S_{\mathrm{S}}},$$

where $\mu_{\max} = 5.56 \times 10^{-5}\,\mathrm{s^{-1}}$, $K_{\mathrm{NO_3}} = 5 \times 10^{-4}\,\mathrm{kg/m^3}$, $K_{\mathrm{S}} = 0.02\,\mathrm{kg/m^3}$. We get

$$\tilde{R}_X = \big(\mu(\boldsymbol{S}) - (1 - f_{\mathrm{P}})b\big) X_{\mathrm{OHO}} Z(X), \quad \tilde{R}_L = R_L^{(2)} = -\left(\frac{\mu(\boldsymbol{S})}{Y} - (1 - f_{\mathrm{P}})b\right) X_{\mathrm{OHO}}.$$

In light of (13), this implies

$$|\mathcal{R}(\boldsymbol{C}, \boldsymbol{S})| \le \left(\mu_{\max} \left|\frac{1}{\rho_X} - \frac{1}{\rho_L Y}\right| + (1 - f_{\mathrm{P}})b \left|\frac{1}{\rho_X} - \frac{1}{\rho_L}\right|\right) X_{\mathrm{m}} = 7.0792 \times 10^{-7}\,\mathrm{m/s},$$

so that q^{reac} is negligibly small in comparison to the bulk velocities q_{e} and q_{u} in continuous sedimentation. It is also negligible in batch sedimentation (although $q_{\mathrm{e}} = q_{\mathrm{u}} = 0$), where the interval of settling velocities is $[0, v_0]$ with $v_0 = 1.76 \times 10^{-3}\,\mathrm{m/s}$.

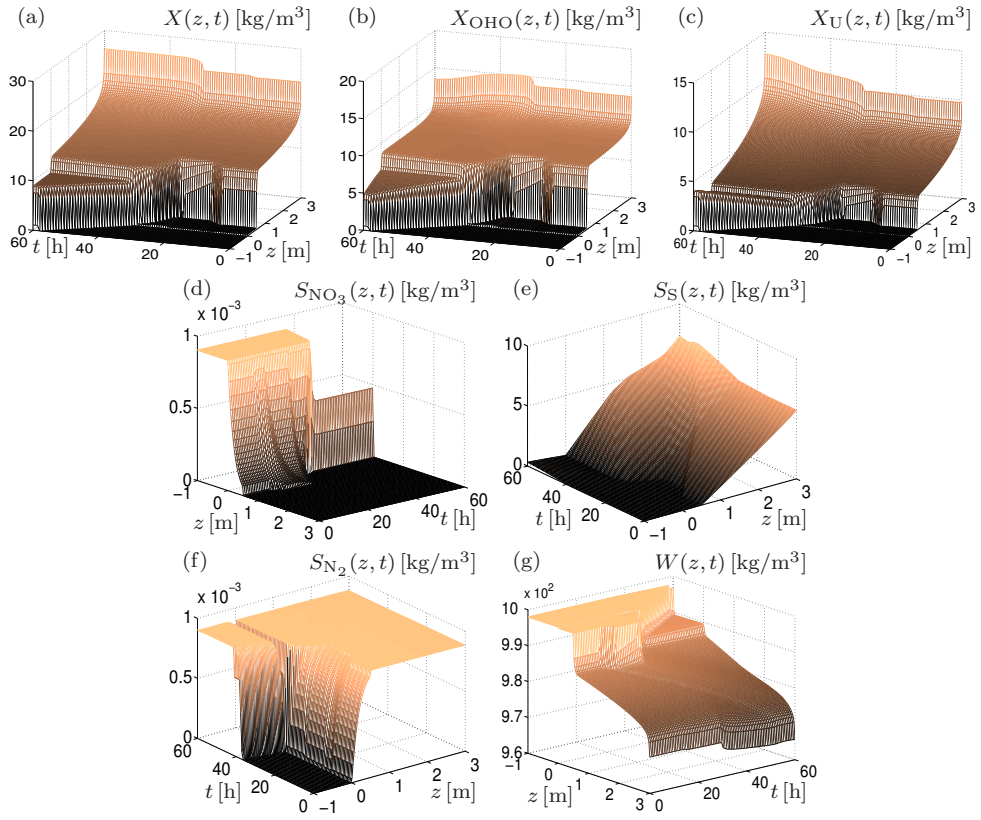

FIG. 3. *Example 1: simulation of reactive settling in an SST starting from a stationary state followed by variations of the volumetric flows Q_{u} and Q_{f} and of the solids feed concentration X_{f}. Here and in Figure 5, the solution displayed is the reference solution obtained with $N = N_{\mathrm{ref}} = 2430$ projected onto a coarser visual grid, and plots (d) and (g) have been rotated.*

The simulations in both examples start from a steady state obtained by a long simulation with $Q_{\mathrm{f}} = 800\,\mathrm{m^3/h}$, $Q_{\mathrm{f}} = 155.6\,\mathrm{m^3/h}$, and the feed inputs $X_{\mathrm{f}} = 5.65\,\mathrm{kg/m^3}$, $\boldsymbol{p}_{X,\mathrm{f}} = (5/7, 2/7)^{\mathrm{T}}$, $S_{\mathrm{S,f}} = 9.00 \times 10^{-4}\,\mathrm{kg/m^3}$, $S_{\mathrm{NO_3,f}} = 6.00 \times 10^{-3}\,\mathrm{kg/m^3}$, and $S_{\mathrm{N_2,f}} = 0\,\mathrm{kg/m^3}$. For both examples the simulation time is $T = 60\,\mathrm{h}$, and the values of N and corresponding time steps Δt determined from (CFL) are given in Table 1.

5.2. Example 1: variations of feed flow and particle concentration. We choose the volume flows $Q_{\mathrm{f}}(t)$, $Q_{\mathrm{u}}(t)$ and the feed concentration $X_{\mathrm{f}}(t)$ as piecewise constant functions of time specified in Figures 2 (a) and (b), respectively, and we let $\boldsymbol{p}_{X,\mathrm{f}}$ and $\boldsymbol{p}_{L,\mathrm{f}}$ be constant in time. We have chosen these extreme variations to test the scheme. The initial steady state is kept during the first 11 h of the simulation; see Figure 3. There is a sludge blanket, i.e., a discontinuity from a low concentration up to the critical concentration $X_{\mathrm{c}} = 5\,\mathrm{kg/m^3}$ separating the hyperbolic and parabolic regions; see also Figure 4 (a). The movement of this discontinuity is of particular interest to model in wastewater treatment. Below the sludge blanket level, the solution is continuous; however, with steep increases just below the sludge blanket and near the bottom. The simulation results show that around $t = 60\,\mathrm{h}$ the SST becomes overloaded with particles leaving also through the effluent. The low volumetric underflow

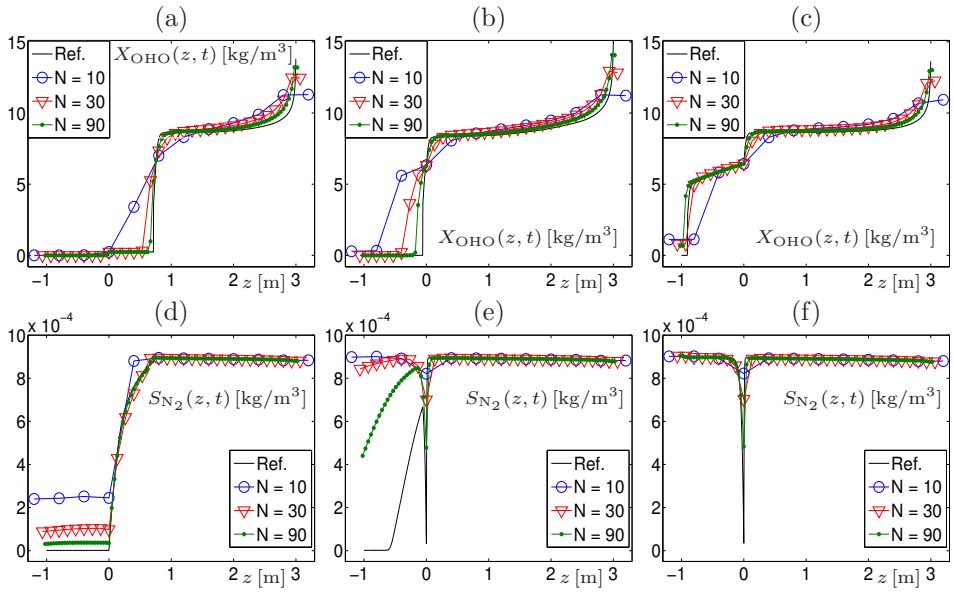

FIG. 4. *Example 1: numerical solutions for coarse discretizations ($N = 10, 30, 90$) at (a, d) $t = 18$ h, (b, e) $t = 36$ h, (c, f) $t = 56$ h. The reference solution ($N = N_{\mathrm{ref}} = 2430$) is included.*

$Q_{\mathrm{u}}(t)$ for $t > 30$ h implies that the soluble nitrate (NO_3) is quickly converted to N_2; see the peak near $z = 0$ in Figure 3 (d) and the corresponding dip in Figure 3 (f) and Figure 4 (e) and (f).

5.3. Example 2: variations of the feed percentages. In this case $Q_{\mathrm{f}}, Q_{\mathrm{u}}$, X_{f} and $\boldsymbol{p}_{L,\mathrm{f}}$ are kept the same constants as for the initial steady-state solution. Only $\boldsymbol{p}_{X,\mathrm{f}}(t)$ is chosen as a piecewise constant function of time as shown in Figure 2 (c). The resulting transportations through the SST of the discontinuities of the solid components are shown in Figure 5 (b) and (c). A part of the incoming nitrate is transported upwards to the effluent without undergoing any reaction since there is no solids in the clarification zone. The lower concentration $X_{\mathrm{OHO,f}}(t)$ for $t \in (15, 20)$ h implies that some nitrate can be seen below the feed level before it disappears; see plot (d).

5.4. Approximate errors. For a given spatial discretization $\Delta z = (B+H)/N$, we denote by $X_{\mathrm{OHO},N}$ the piecewise constant function with $X_{\mathrm{OHO},N}(z,t) = P^{(1),n}_{X,j} X^n_j$ if $z \in (z_{j-1/2}, z_{j+1/2}]$ and $t \in (t_{n-1}, t_n]$, and define the approximate relative L^1 error

$$e^{\mathrm{rel}}_{N,X_{\mathrm{OHO}}}(t) := \left\| (X_{\mathrm{OHO},N} - X_{\mathrm{OHO},N_{\mathrm{ref}}})(\cdot,t) \right\|_{L^1(-H,B)} / \left\| X_{\mathrm{OHO},N_{\mathrm{ref}}}(\cdot,t) \right\|_{L^1(-H,B)},$$

where $N_{\mathrm{ref}} = 2430$. The corresponding quantities for X_{U}, $S_{\mathrm{NO_3}}$, $S_{\mathrm{N_2}}$ and S_{S} are defined in the same way. We define the total approximate relative error

$$e^{\mathrm{rel}}_N(t) := e^{\mathrm{rel}}_{N,X_{\mathrm{OHO}}}(t) + e^{\mathrm{rel}}_{N,X_{\mathrm{U}}}(t) + e^{\mathrm{rel}}_{N,S_{\mathrm{NO_3}}}(t) + e^{\mathrm{rel}}_{N,S_{\mathrm{N_2}}}(t) + e^{\mathrm{rel}}_{N,S_{\mathrm{S}}}(t)$$

and the observed convergence rate between two discretizations $N = N_1$ and $N = N_2$,

$$\theta(t) := -\log\left(e^{\mathrm{rel}}_{N_1}(t)/e^{\mathrm{rel}}_{N_2}(t)\right)/\log(N_1/N_2).$$

Table 2 shows values of $e^{\mathrm{rel}}_N(t)$ and $\theta(t)$, along with corresponding CPU times, for Examples 1 and 2 at the times used in Figures 4 and 6. We observe that all approximate

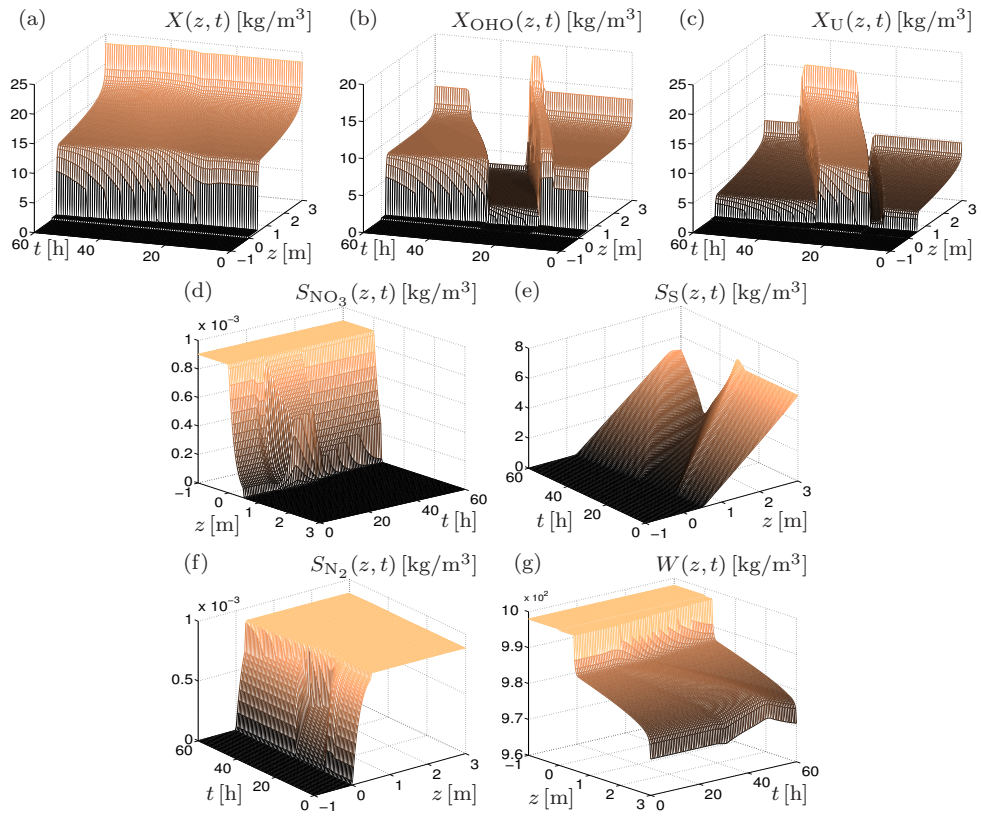

FIG. 5. *Example 2: simulation of reactive settling in an SST starting from a stationary state followed by variations of the feed percentages of the substrates.*

total relative errors tend to zero as N is increased. The rates θ assume values between zero and one for $N \leq 405$ (among the selected values of N), as should be expected for a first-order discretization in time and for the convective flux (see [8, 9] for comparable results). The values $\theta > 1$ observed for $N_1 = 405$ and $N_2 = 810$ do, however, alert to the limitations of error analysis via a reference solution with $N_{\mathrm{ref}} = 2430$.

6. Concluding remarks. The one-dimensional model equations (1) for continuous sedimentation of multi-component solid particles in a liquid, containing several soluble constituents, with possible biochemical reactions have been derived. Previous model ingredients such as hindered settling and compression at high concentrations have been complemented with the transport and reactions of components. Focus has been laid on the application to wastewater treatment, for which special simplifying model assumptions facilitate the (partial) mathematical analysis. One assumption is that the solid and liquid phases each has a constant density. This is not restrictive in wastewater treatment, where the concentrations of the soluble substrates are negligible in comparison to the water component. The technical assumptions (7) were made to guarantee a bounded solution. We believe, however, that the solution is bounded for realistic reaction terms in each application without (7).

Although there are only two densities, their difference and the reactions cause

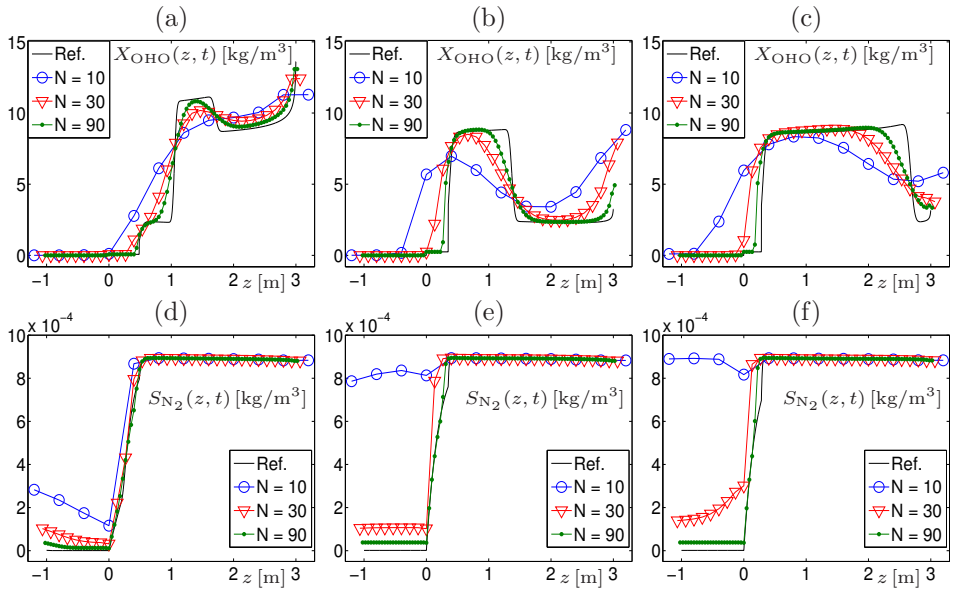

FIG. 6. *Example 2: numerical solutions for coarse discretizations ($N = 10, 30, 90$) at (a, c) $t = 18$ h, (b, d) $t = 36$ h an (e, f) $t = 46$ h. The reference solution ($N = N_{\mathrm{ref}} = 2430$) is included.*

TABLE 2
Total approximate relative L^1 errors $e_N^{\mathrm{rel}}(t)$, convergence rates $\theta(t)$ and CPU times cpu *for Examples 1 (top) and 2 (bottom) measured for the indicated simulated time.*

	Example 1, $t = 18$ h			Example 1, $t = 36$ h			Example 1, $t = 56$ h		
N	$e_N^{\mathrm{rel}}(t)$	$\theta(t)$	cpu [s]	$e_N^{\mathrm{rel}}(t)$	$\theta(t)$	cpu [s]	$e_N^{\mathrm{rel}}(t)$	$\theta(t)$	cpu [s]
10	0.555	—	1.20	0.840	—	2.16	0.384	—	3.83
30	0.251	0.721	2.68	0.543	0.396	5.41	0.191	0.634	8.82
90	0.103	0.815	7.57	0.315	0.497	15.85	0.103	0.567	31.70
270	0.037	0.932	22.15	0.122	0.859	44.99	0.048	0.698	81.66
405	0.025	0.999	44.20	0.087	0.847	69.21	0.033	0.928	127.95
810	0.010	1.288	108.52	0.032	1.443	162.57	0.013	1.316	269.23
	Example 2, $t = 18$ h			Example 2, $t = 36$ h			Example 2, $t = 46$ h		
N	$e_N^{\mathrm{rel}}(t)$	$\theta(t)$	cpu [s]	$e_N^{\mathrm{rel}}(t)$	$\theta(t)$	cpu [s]	$e_N^{\mathrm{rel}}(t)$	$\theta(t)$	cpu [s]
10	0.766	—	1.19	1.70	—	2.15	1.555	—	2.90
30	0.363	0.679	2.71	0.668	0.852	5.41	0.717	0.704	6.83
90	0.184	0.620	7.63	0.259	0.862	15.24	0.286	0.836	19.34
270	0.081	0.751	22.21	0.096	0.905	44.45	0.115	0.831	56.68
405	0.056	0.893	34.14	0.065	0.969	95.57	0.079	0.922	86.62
810	0.027	1.046	80.29	0.029	1.180	186.21	0.036	1.119	203.92

a volume change of the suspension; see the bulk velocity component due to reactions q^{reac} of the total bulk velocity q in (18). In wastewater treatment, q^{reac} seems to be negligible. Hence, our numerical scheme will produce very similar solutions when setting $q^{\mathrm{reac}} = 0$. The latter was, however, done to obtain a three-point explicit scheme with the monotonicity properties that lead to the invariant region property; see Theorem 2. For other applications with larger q^{reac}, our scheme can still be used. This case will be studied in the future.

While this paper is focused on the model formulation, the development of a numerical scheme and its applications, the well-posedness analysis is still open. The basic

difficulties associated with the model (1) are discussed in Section 1.2. The numerical results confirm that solutions are discontinuous due to changes in the definitions of fluxes across the inlet $z = 0$ and outlets $z = -H, B$ (visible, for instance, in Figure 3 (a) at $z = 0$), the nonlinearity of the flux as a function of X, and the strongly degenerating behaviour of D. The combined effect of both becomes visible, for instance, in the sharpness of the solution at the typical sludge blanket in Figure 3 (a), which moves up into the clarification zone and eventually overloads the SST. Moreover, the invariant region principle (Theorem 2) is not only an asset in itself for practical purposes (concentrations are nonnegative and percentages satisfy their natural requirements, properties that are not automatically built into finite volume schemes [25]), but along with the underlying monotonicity could also form an important step towards proving existence of a weak solution of the problem via convergence of a scheme, as was done in [8, 9, 27] and many other works for related problems.

Finally, a more thorough study of the relative influence of the convective, diffusive (compressive), and reactive terms is required. For instance, in our examples Δt (in Table 1) is almost constant for $N \leq 405$, which comes from the dominance of $\beta_{\boldsymbol{P}_L}$, and as a consequence, for fixed t the CPU time depends almost linearly on N for $N \leq 405$ (cf. Table 2). In a more diffusion (compression)-dominant scenario, with substantially larger values of $\|d\|_\infty$ and thus of β_X, the $\mathcal{O}(N^3)$ increase of CPU time with N (for fixed t) stipulated by (CFL) and (37) would become noticeable at much smaller values of N. One should therefore develop more efficient solvers for the model, for example a semi-implicit variant of the scheme that would limit this growth to $\mathcal{O}(N^2)$.

REFERENCES

[1] J. Alex, S. G. E. Rönner-Holm, M. Hunze, and N. C. Holm, *A combined hydraulic and biological SBR model*, Wat. Sci. Tech., 64 (2011), pp. 1025–1031.

[2] T. Arbogast, C.-S. Huang, and T. F. Russell, *A locally conservative Eulerian–Lagrangian method for a model two-phase flow problem in a one-dimensional porous medium*, SIAM J. Sci. Comput., 34 (2012), pp. A1950–A1974.

[3] S. Borazjani, A. J. Roberts, and P. Bedrikovetsky, *Splitting in systems of PDEs for two-phase multicomponent flow in porous media*, Appl. Math. Letters, 53 (2016), pp. 25–32.

[4] R. Bürger, J. Careaga, S. Diehl, C. Mejías, I. Nopens, and P. A. Vanrolleghem, *Simulations of reactive settling of activated sludge with a reduced biokinetic model.* To appear in Computers Chem. Eng., 2016.

[5] R. Bürger, S. Diehl, S. Farås, I. Nopens, and E. Torfs, *A consistent modelling methodology for secondary settling tanks: A reliable numerical method*, Water Sci. Tech., 68 (2013), pp. 192–208.

[6] R. Bürger, S. Diehl, and I. Nopens, *A consistent modelling methodology for secondary settling tanks in wastewater treatment*, Water Res., 45 (2011), pp. 2247–2260.

[7] R. Bürger, R. Donat, P. Mulet, and C. A. Vega, *Hyperbolicity analysis of polydisperse sedimentation models via a secular equation for the flux Jacobian*, SIAM J. Appl. Math., 70 (2010), pp. 2186–2213.

[8] R. Bürger, K. H. Karlsen, N. H. Risebro, and J. D. Towers, *Well-posedness in BV_t and convergence of a difference scheme for continuous sedimentation in ideal clarifier-thickener units*, Numer. Math., 97 (2004), pp. 25–65.

[9] R. Bürger, K. H. Karlsen, and J. D. Towers, *A model of continuous sedimentation of flocculated suspensions in clarifier-thickener units*, SIAM J. Appl. Math., 65 (2005), pp. 882–940.

[10] J.-P. Chancelier, M. C. de Lara, and F. Pacard, *Analysis of a conservation PDE with discontinuous flux: A model of settler*, SIAM J. Appl. Math., 54 (1994), pp. 954–995.

[11] S. Diehl, *On scalar conservation laws with point source and discontinuous flux function*, SIAM J. Math. Anal., 26 (1995), pp. 1425–1451.

[12] S. Diehl, *A conservation law with point source and discontinuous flux function modelling continuous sedimentation*, SIAM J. Appl. Math., 56 (1996), pp. 388–419.

[13] S. Diehl, *Scalar conservation laws with discontinuous flux function:* I. *The viscous profile*

condition, Commun. Math. Phys., 176 (1996), pp. 23–44.
[14] S. Diehl, *Continuous sedimentation of multi-component particles*, Math. Meth. Appl. Sci., 20 (1997), pp. 1345–1364.
[15] S. Diehl, *Dynamic and steady-state behaviour of continuous sedimentation*, SIAM J. Appl. Math., 57 (1997), pp. 991–1018.
[16] S. Diehl, *A uniqueness condition for nonlinear convection-diffusion equations with discontinuous coefficients*, J. Hyperbolic Differential Equations, 6 (2009), pp. 127–159.
[17] S. Diehl and N.-O. Wallin, *Scalar conservation laws with discontinuous flux function: II. On the stability of the viscous profiles*, Commun. Math. Phys., 176 (1996), pp. 45–71.
[18] D. A. Drew and S. L. Passman, *Theory of Multicomponent Fluids*, vol. 135, Springer-Verlag, New York, 1999.
[19] X. Flores-Alsina, K. Gernaey, and U. Jeppsson, *Benchmarking biological nutrient removal in wastewater treatment plants: Influence of mathematical model assumptions*, Water Sci. Tech., 65 (2012), pp. 1496–1505.
[20] K. V. Gernaey, U. Jeppsson, D. J. Batstone, and P. Ingildsen, *Impact of reactive settler models on simulated WWTP performance*, Water Sci. Tech., 53 (2006), pp. 159–167.
[21] T. Gimse and N. H. Risebro, *Solution of the Cauchy problem for a conservation law with a discontinuous flux function*, SIAM J. Math. Anal., 23 (1992), pp. 635–648.
[22] J. M. N. T. Gray and C. Ancey, *Multi-component particle-size segregation in shallow granular avalanches*, J. Fluid Mech., 678 (2011), pp. 535–588.
[23] J. Guerrero, X. Flores-Alsina, A. Guisasola, J. A. Baeza, and K. V. Gernaey, *Effect of nitrite, limited reactive settler and plant design configuration on the predicted performance of simultaneous C/N/P removal WWTPs*, Bioresource Tech., 136 (2013), pp. 680–688.
[24] J. Hamilton, R. Jain, P. Antoniou, S. A. Svoronos, B. Koopman, and G. Lyberatos, *Modeling and pilot-scale experimental verification for predenitrification process*, J. Environ. Eng., 118 (1992), pp. 38–55.
[25] S. Jaouen and F. Lagoutière, *Numerical transport of an arbitrary number of components*, Computer Methods Appl. Mech. Eng., 196 (2007), pp. 3127–3140.
[26] K. H. Karlsen and N. H. Risebro, *On the uniqueness and stability of entropy solutions of nonlinear degenerate parabolic equations with rough coefficients*, Discrete Continuous Dynamical Systems, 9 (2003), pp. 1081–1104.
[27] K. H. Karlsen, N. H. Risebro, and J. D. Towers, *Upwind difference approximations for degenerate parabolic convection-diffusion equations with a discontinuous coefficient*, IMA J. Numer. Anal., 22 (2002), pp. 623–664.
[28] K. H. Karlsen, N. H. Risebro, and J. D. Towers, *L^1 stability for entropy solutions of nonlinear degenerate parabolic convection-diffusion equations with discontinuous coefficients*, Trans. Royal Norwegian Society Sci. Letters (Skr. K. Nor. Vidensk. Selsk.), 3 (2003), p. 49.
[29] B. Li and M. K. Stenstrom, *Practical identifiability and uncertainty analysis of the one-dimensional hindered-compression continuous settling model*, Water Res., 90 (2016), pp. 235–246.
[30] Z. Li, R. Qi, B. Wang, Z. Zou, G. Wei, and M. Yang, *Cost-performance analysis of nutrient removal in a full-scale oxidation ditch process based on kinetic modeling*, J. Environ. Sci., 25 (2013), pp. 26–32.
[31] G. S. Ostace, V. M. Cristea, and P. S. Agachi, *Evaluation of different control strategies of the waste water treatment plant based on a modified activated sludge model no. 3*, Environ. Eng. Management J., 11 (2012), pp. 147–164.
[32] J. F. Richardson, J. H. Harker, and J. R. Backhurst, *Chemical Engineering, Particle Technology and Separation Processes*, vol. 2, Butterworth-Heinemann, fifth ed., 2002.
[33] V. V. Shelukhin, *Quasistationary sedimentation with adsorption*, J. Appl. Mech. Tech. Phys., 46 (2005), pp. 513–522.
[34] L. Svarovsky, *Countercurrent washing of solids*, in Solid-Liquid Separation, L. Svarovsky, ed., Butterworth-Heinemann, Oxford, fourth edition ed., 2001, ch. 15, pp. 442–475.
[35] E. Torfs, T. Maere, R. Bürger, S. Diehl, and I. Nopens, *Impact on sludge inventory and control strategies using the benchmark simulation model no. 1 with the Bürger-Diehl settler model*, Water Sci. Tech., 71 (2015), pp. 1524–1535.

Centro de Investigación en Ingeniería Matemática (CI^{2}MA)

PRE-PUBLICACIONES 2016

2016-06 Anahi Gajardo, Vincent Nesme, Guillaume Theyssier: *Pre-expansivity in cellular automata*

2016-07 Eligio Colmenares, Michael Neilan: *Dual-mixed finite element methods for the stationary Boussinesq problem*

2016-08 Veronica Anaya, David Mora, Carlos Reales, Ricardo Ruiz-Baier: *Finite element methods for a stream-function – vorticity formulation of the axisymmetric Brinkman equations*

2016-09 Rommel Bustinza, Bibiana López-Rodríguez, Mauricio Osorio: *An a priori error analysis of an HDG method for an eddy current problem*

2016-10 Luis M. Castro, Víctor H. Lachos, Tsung-I Lin, Larissa A. Matos: *Heavy-tailed longitudinal regression models for censored data: A likelihood based perspective*

2016-11 Gabriel N. Gatica, Ricardo Ruiz-Baier, Giordano Tierra: *A posteriori error analysis of an augmented mixed method for the Navier-Stokes equations with nonlinear viscosity*

2016-12 Manuel Solano, Felipe Vargas: *A high order HDG method for Stokes flow in curved domains*

2016-13 Huangxin Chen, Weifeng Qiu, Ke Shi, Manuel Solano: *A superconvergent HDG method for the Maxwell equations*

2016-14 Lourenco Beirao-Da-Veiga, David Mora, Gonzalo Rivera: *A virtual element method for Reissner-Mindlin plates*

2016-15 Rodolfo Araya, Christopher Harder, Abner Poza, Frederic Valentin: *Multiscale hybrid-mixed method for the Stokes and Brinkman equations - The method*

2016-16 Luis M. Castro, José González, Víctor H. Lachos, Alexandre Patriota: *A confidence set analysis for observed samples: A fuzzy set approach*

2016-17 Raimund Bürger, Stefan Diehl, Camilo Mejías: *A model of continuous sedimentation with compression and reactions*

Para obtener copias de las Pre-Publicaciones, escribir o llamar a: Director, Centro de Investigación en Ingeniería Matemática, Universidad de Concepción, Casilla 160-C, Concepción, Chile, Tel.: 41-2661324, o bien, visitar la página web del centro: `http://www.ci2ma.udec.cl`







Centro de Investigación en
Ingeniería Matemática (CI²MA)
Universidad de Concepción

Casilla 160-C, Concepción, Chile
Tel.: 56-41-2661324/2661554/2661316
http://www.ci2ma.udec.cl